0021-972X/07/$15.00/0
Printed in U.S.A.

The Journal of Clinical Endocrinology & Metabolism 92(2):532–541

doi: 10.1210/jc.2006-1546

Efficacy and Safety of Leptin-Replacement Therapy and Possible Mechanisms of Leptin Actions in Patients with Generalized Lipodystrophy

Ken Ebihara, Toru Kusakabe, Masakazu Hirata, Hiroaki Masuzaki, Fumiko Miyanaga, Nozomi Kobayashi, Tomohiro Tanaka, Hideki Chusho, Takashi Miyazawa, Tatsuya Hayashi, Kiminori Hosoda, Yoshihiro Ogawa, Alex M. DePaoli, Masanori Fukushima, and Kazuwa Nakao

Department of Medicine and Clinical Science (K.E., T.K., M.H., H.M., F.M., N.K., T.T., H.C., T.M., T.H., K.H., Y.O., K.N.), Kyoto University Graduate School of Medicine, and Department of Clinical Trial Management (M.F.), Translational Research Center, Kyoto University Hospital, Kyoto 606-8507, Japan; and Amgen Inc. (A.M.D.), Thousand Oaks, California 91319

Background: Lack of leptin is implicated in insulin resistance and other metabolic abnormalities in generalized lipodystrophy; however, the efficacy, safety, and underlying mechanisms of leptin-replacement therapy in patients with generalized lipodystrophy remain unclear.

Methods: Seven Japanese patients with generalized lipodystrophy, two acquired and five congenital type, were treated with the physiological replacement dose of recombinant leptin during an initial 4-month hospitalization followed by outpatient follow-up for up to 36 months.

Results: The leptin-replacement therapy with the twice-daily injection dramatically improved fasting glucose (mean ± SE, 172 ± 20 to 120 ± 12 mg/dl, $P < 0.05$) and triglyceride levels (mean ± SE, 700 ± 272 to 260 ± 98 mg/dl, $P < 0.05$) within 1 wk. The leptin-replacement therapy reduced insulin resistance evaluated by euglycemic clamp method and augmented insulin secretion at glucose tolerance test with different responses between acquired and congenital types. Improvement of the fatty liver was also observed. The efficacy and safety of the once-daily injection were comparable to those of the twice-daily injection. The leptin-replacement therapy ameliorated macro- and microalbuminuria and showed no deterioration of neuropathy and retinopathy of these patients. The leptin-replacement therapy is beneficial to diabetic complications and lipodystrophic ones. Two patients developed antileptin antibodies but not neutralizing antibodies. The therapy was well tolerated, and its effects were maintained for up to 36 months without any notable adverse effects such as hypoglycemia, high blood pressure, or reduction of bone mineral density.

Conclusions: The present study demonstrates the efficacy and safety of the long-term leptin-replacement therapy and possible mechanisms of leptin actions in patients with generalized lipodystrophy. (*J Clin Endocrinol Metab* **92: 532–541, 2007**)

LEPTIN PLAYS A MAJOR role in the regulation of energy homeostasis (1). The plasma leptin concentration increases in proportion to the degree of adiposity (2–6). Besides the antiobesity actions, leptin has a wide range of actions including antidiabetic actions (6–8).

Generalized lipodystrophy is a heterogeneous group of diseases characterized by a profound deficiency of adipose tissue (9) and is commonly associated with severe insulin-resistant diabetes, hypertriglyceridemia, and fatty liver (10, 11). In lipoatrophic patients, these metabolic abnormalities develop as a consequence of decreased mass of the adipose tissue (12–14), and consequently, plasma leptin concentrations are markedly reduced (15). We and others demonstrated that the leptin administration or transgenic overexpression of leptin reverses the metabolic abnormalities in different mouse models of lipodystrophy, indicating that the metabolic abnormalities in lipoatrophic patients are caused mainly by a shortage of leptin (16, 17). Recently, the 4-month leptin-replacement therapy with twice-daily injection protocol was reported to improve glucose and lipid metabolism in nine female patients with lipodystrophy in the United States (18).

In the present study, we evaluated the efficacy and safety of long-term leptin-replacement therapy on seven Japanese patients with generalized lipodystrophy.

First Published Online November 21, 2006

Abbreviations: AGL, Acquired generalized lipodystrophy; CGL, congenital generalized lipodystrophy; CT, computed tomography; HbA1c, glycosylated hemoglobin; L/S, liver to spleen; r-metHuLeptin, recombinant methionyl human leptin.

Subjects and Methods

Subjects

Eligible criteria were according to the study protocol of the National Institutes of Health (18). We evaluated seven patients with generalized lipodystrophy including two patients with acquired generalized lipodystrophy (AGL) and five patients with congenital generalized lipodystrophy (CGL). Patients with CGL were further analyzed for mutations in either *seipin* (19) or 1-acylglycerol-3-phosphate *O*-acyltransferase2 (*AGPAT2*) genes (20). Table 1 summarizes the baseline clinical characteristics of seven patients treated in the present study.

Study design

The study protocol was approved by the ethical committee of Kyoto University Graduate School of Medicine (approval number 331). Informed written consent was obtained from all subjects and their families. Recombinant methionyl human leptin (r-metHuLeptin) was provided by Amgen, Inc. (Thousand Oaks, CA). For the first year, r-metHuLeptin

TABLE 1. Characteristics of the patients at baseline

Patient no.	1	2	3	4	5	6	7	Mean ± SE
Age (yr)	11	29	19	16	15	23	33	21 ± 3
Sex	F	M	M	F	F	F	F	
Type of lipodystrophy	AGL	CGL[a]	CGL[b]	AGL	CGL[b]	CGL[b]	CGL[a]	
Body weight (kg)	31.0	32.0	52.8	34.6	43.5	52.0	53.9	42.8 ± 3.9
BMI (kg/m^2)	16.0	14.2	19.7	13.9	17.9	21.2	20.3	17.6 ± 1.1
Body fat (%)[c]	5.0	4.7	5.0	5.8	5.4	5.7	10.0	5.9 ± 0.7
Age of DM onset (yr)	9	11	10	15	6	5	14	10 ± 1
Duration of DM (yr)	2	18	9	1	9	18	19	11 ± 3
Leptin (ng/ml)	0.92	0.82	1.23	1.15	0.90	1.23	1.40	1.09 ± 0.08
Fasting glucose (mg/dl)	208	142	105	138	247	221	130	172 ± 21
HbA1c (%)	10.0	10.3	8.8	7.9	7.7	10.2	10.2	9.3 ± 0.4
Triglyceride (mg/dl)	1941	69	1031	1246	89	254	232	695 ± 273
Total cholesterol (mg/dl)	250	183	194	298	185	285	233	233 ± 18
L/S ratio	0.78	1.23	0.95	0.35	1.12	0.88	0.73	0.86 ± 0.11
Urinary albumin (mg/d)	48.4	6.9	31.0	778	20.3	359	11.3	179.3 ± 110.5
Blood pressure (mm Hg)	114/48	120/82	126/54	92/52	108/56	104/64	108/70	110 ± 4/61 ± 5
Bone mineral density (g/cm^2)[c]	0.94	0.88	1.32	0.90	1.06	1.37	1.33	1.11 ± 0.08
Diet therapy (kcal/d)	1500	1500	1800	1500	1500	1600	1500	
Antidiabetic therapy	Pioglitazone (15 mg/d)	Glibenclamide (2.5 mg/d), voglibosie (0.6 mg/d)	Insulin (60 IU/d)	Pioglitazone (30 mg/d)	None	Pioglitazone (45 mg/d)	Insulin (20 U/d)	
Lipid-lowering therapy	None	None	None	Pravastatin (40 mg/d), bezafibrate (400 mg/d)	None	None	None	

BMI, Body mass index; DM, diabetes mellitus; L/S ratio, ratio of liver to spleen for CT attenuation values.
[a] CGL due to neither *seipin* nor *AGPAT2* mutation.
[b] CGL due to *seipin* mutation.
[c] Body fat and bone mineral density were measured by dual energy x-ray absorptiometry.

was administered as twice-daily sc injection (18). The physiological replacement dose was estimated to be 0.02 mg/kg·d for men, 0.03 mg/kg·d for girls under 18 yr of age, and 0.04 mg/kg·d for women on the basis of information provided by Amgen. Patient 1 was treated with 100% of the replacement dose for the entire period. Patient 2 was treated with 100% for the first and second month and 200% thereafter. Patients 3–7 were treated with 50% for the first month, 100% for the second month, and 200% thereafter. All patients were evaluated as inpatients for the first 4 months. After discharge, patients attended local clinics for every leptin injection, and all of the leptin injections were done by medical doctors because self-injection of r-metHuLeptin, which was not approved as a drug, was not permitted in Japan. Each patient had been prescribed a diet of fixed calories indicated in Table 1 beginning at least 2 months before the initiation of leptin-replacement therapy, and this was not altered throughout the therapy. The dose of antidiabetic and lipid-lowering drugs was tapered or the treatment discontinued as needed. After 12 months of twice-daily leptin treatment, we reduced the dosing frequency to once daily without change of total daily dose. At present, total duration of leptin-replacement therapy was 36 months for patient 1 and 2, 24 months for patient 3, 18 months for patient 4, 8 months for patient 5, and 2 months for patients 6 and 7.

Biochemical analysis

Plasma leptin levels were determined by the immunoassay (Linco, St. Charles, MO). Plasma glucose, serum triglycerides, total cholesterol, alanine aminotransferase, aspartate aminotransferase, and serum and urine creatinine levels were determined according to standard methods with the use of automated equipment. Glycosylated hemoglobin (HbA1c) levels were measured by ion-exchange HPLC. Serum insulin levels were determined by immunoassays (Shibayagi Co., Ltd., Gunma, Japan). Urine albumin excretion was assayed with a human albumin ELISA kit (Sanko Junyaku Co., Ltd., Tokyo, Japan). Antibodies to leptin in serum was tested with the use of a solid-phase RIA, and the potential neutralizing effects of antibodies on leptin bioactivity were assessed in an *in vitro* bioassay developed by Amgen (Thousand Oaks, CA) (21).

Procedures

Body fat and whole-body bone mineral density were determined by dual-energy x-ray absorptiometry (QDR-2000; Hologic Inc., Bedford, MA). The oral glucose tolerance test (75 g) was performed after an overnight fast. In patients under insulin therapy, insulin injection was stopped from the previous night. The Σ values of plasma glucose (PG) levels and serum insulin (IRI) levels were calculated by the sum of the values at 0, 30, 60, 90, 120, and 180 min after administration. Insulin action on glucose uptake in peripheral tissues was evaluated using the hyperinsulinemic-euglycemic glucose clamp technique (22). Fatty liver was diagnosed by both ultrasound and computed tomography (CT) imaging. Liver volume was calculated with the use of CT imaging. Lipid contents of liver and skeletal muscle were determined by magnetic resonance imaging performed on a 1.5-T system (Magnetom Symphony; Siemens Medical System, Erlangen, Germany). The signal intensity of the same region on both the in-phase image (I_{in}) and the out-of-phase image (I_{out}) was measured. The fat index (FI) was defined by the following formulae: $FI = (I_{in} - I_{out}) / I_{in}$. Tissue lipid content was calculated using FI as previously reported (23).

Statistical analysis

Data were expressed as the mean ± SE. Comparison between baseline data and data obtained at various times was assessed by ANOVA and completed by Fisher's probable least-significant difference test, as required.

Results

Baseline characteristics

Three of five CGL patients were homozygous for the same nonsense mutation (R275X) of the *seipin* gene as we previously reported (Table 1) (24). The remaining CGL patients had neither *seipin* nor *AGPAT2* gene mutation (24, 25). All the patients had markedly decreased body fat, hypoleptinemia, and uncontrolled diabetes with high fasting glucose levels and HbA1c levels, despite the diet and exercise therapy and the use of oral antidiabetic drugs or insulin. Their age of onset and duration of diabetes are also summarized in Table 1. Three of seven patients had marked fasting hypertriglyceridemia at the level above 1000 mg/dl. The mean ± SE of the total cholesterol level was 233 ± 18 mg/dl. Five patients were diagnosed to have fatty liver, and their ratios of liver to spleen (L/S ratio) for CT attenuation values were under 0.95. Four of seven patients had elevated urine albumin excretion (>30 mg/d), and two of them had macroalbuminuria (>300 mg/d). All the patients showed normal blood pressure (mean ± SE, 110 ± 4/61 ± 5 mm Hg) and bone mineral density (mean ± SE, 1.11 ± 0.08 g/cm^2).

High compliance of leptin-replacement therapy

All of the leptin injections were done by medical doctors. For the initial 4 months, all the patients received 100% of scheduled leptin injections as inpatients. After discharge, patients attended local clinics for every leptin injection and received over 98% as outpatients thereafter.

Achievement of physiological replacement of leptin

At any dose, peak plasma levels occurred 2 h after the leptin injection. The peak plasma leptin levels at the doses of 50, 100, and 200% under the protocol of twice-daily injections were 4.05 ± 0.19, 9.80 ± 1.70, 18.95 ± 1.58 (mean ± SE) ng/ml, respectively. The peak plasma leptin level of the 400% dose under the protocol of once-daily injections was 34.48 ± 2.11 (mean ± SE) ng/ml. Thus, the elevations of plasma leptin level were dose dependent, and physiological replacement was achieved as expected.

Rapid effects on glucose and triglyceride levels

The fasting plasma glucose levels decreased day by day in all the patients, and a significant reduction was achieved within 7 d (mean ± SE, 172 ± 20 mg/dl at baseline *vs.* 120 ± 12 mg/dl after 7 d, $P < 0.05$) (Table 2). By 4 months, all the patients, except patient 6, were able to discontinue all of the antidiabetic drugs (Table 1). Patient 6 could reduce the dose of the antidiabetic drug by 2 months.

The fasting triglyceride levels also decreased day by day in all the patients, and a significant reduction was achieved within 7 d (mean ± SE, 700 ± 272 mg/dl at baseline *vs.* 260 ± 98 mg/dl after 7 d, $P < 0.05$) (Table 2). Lipid-lowering drugs of patient 4 were able to be discontinued by 4 months.

Glucose tolerance tests

As shown in Fig. 1A, the mean plasma glucose levels in response to the oral 75-g glucose load were dramatically improved already at 1 month and were maintained at 2 and 4 months in all patients. The insulin levels were distinctly low before the treatment in both AGL and CGL patients (Fig. 1, B and C). The changes after the initiation of the leptin-replacement therapy of serum insulin levels showed a marked contrast between AGL and CGL patients. Glucose-induced insulin secretion was dramatically improved already at 1

TABLE 2. Changes of fasting plasma glucose and serum triglyceride levels for first month of the leptin-replacement therapy

Patient no.	Fasting plasma glucose (mg/dl)					Fasting serum triglyceride (mg/dl)				
	Baseline	1 d	3 d	7 d	30 d	Baseline	7 d	14 d	21 d	28 d
1	208	177	160	108	76	1941	653	210	204	218
2	142	115	119	102	94	69	51	49	72	50
3	105	100	89	105	108	1031	122	108	97	115
4	138	125	126	96	108	1246	589	320	425	496
5	247	227	204	182	151	254	399	134	151	194
6	221	185	169	141	130	89	63	54	131	74
7	141	135	133	105	125	269	54	85	95	99
Mean ± SE	172 ± 20	152 ± 17	143 ± 14	120 ± 12[a]	113 ± 9[b]	700 ± 272	260 ± 98[a]	110 ± 38[b]	168 ± 46[b]	178 ± 58[b]

[a] $P < 0.05$ compared to baseline.
[b] $P < 0.01$ compared to baseline.

month in AGL patients (Fig. 1B), whereas no apparent improvement in insulin secretion was observed even after 4 months of the therapy in CGL patients (Fig. 1C). To evaluate the ability of insulin secretion, we calculated the values of ΣIRI/ΣPG in a 75-g oral glucose tolerance test. The values of ΣIRI/ΣPG were substantially increased at 1 month in two AGL patients, and additional increases were observed at 2 and 4 months, whereas those in five CGL patients remained unchanged even after 4 months of the therapy (Fig. 1D).

Hyperinsulinemic-euglycemic clamp study

The glucose infusion rates during the hyperinsulinemic-euglycemic clamp study were distinctly low at baseline in all the patients (mean ± SE, 2.5 ± 0.3 mg/kg·min; range, 1.60–3.6 mg/kg·min). The increase of glucose infusion rate was observed but not statistically significant at 1 month on the treatment (mean ± SE, 3.7 ± 0.3 mg/kg·min, $P = 0.062$ *vs.* at baseline). A significant increase was achieved at 2 months (mean ± SE, 4.4 ± 0.4 mg/kg·min, $P < 0.01$ *vs.* at baseline) and an additional increase was observed at 4 months (mean ± SE, 5.6 ± 1.0 mg/kg·min, $P < 0.001$ *vs.* at baseline). By contrast to insulin secretion, no apparent difference between AGL and CGL patients was observed on the changes of insulin sensitivity.

In patient 4, the hyperinsulinemic-euglycemic clamp study was performed at 10 d. A substantial increase of glucose infusion rate was detected already at 10 d (2.52 mg/kg·min at baseline and 4.63 mg/kg·min at 10 d) and again at 1 month (4.59 mg/kg·min), which was comparable to that at 4 months (5.06 mg/kg·min).

Effects on fatty liver

Five of seven patients were diagnosed to have apparent fatty liver. The L/S ratios of CT attenuation value in five of seven patients were 0.74 ± 0.10 (mean ± SE) (Table 1). The L/S ratio of CT attenuation value in these patients improved from 0.74 ± 0.10 (mean ± SE) to 1.09 ± 0.06 (mean ± SE) by 2 months and further improved thereafter. Consistent with this, in these patients, the alanine aminotransferase level decreased from 80.5 ± 24.2 to 32.3 ± 4.6 U/liter (mean ± SE), and the ASL level decreased from 42.3 ± 11.1 to 21.5 ± 4.3 U/liter (mean ± SE) by 2 months, and these values were also further improved thereafter. The liver volume also decreased in all patients who had fatty liver at baseline (mean ± SE,

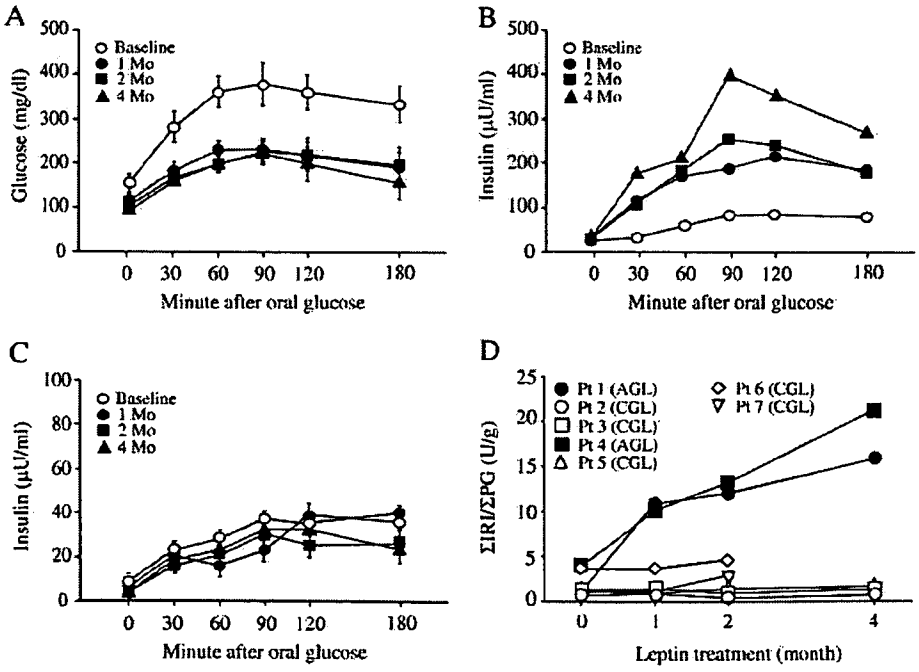

FIG. 1. Mean ± SE plasma glucose levels in all seven patients (A), mean serum insulin levels in two AGL patients (B), mean ± SE serum insulin levels in five CGL patients (C), and ΣIRI/ΣPG of each patient (D) after an oral 75-g glucose-tolerance test before and after 1, 2, and 4 months of the leptin-replacement therapy. ΣIRI, Sum of the plasma insulin levels before and 30, 60, 90, 120, and 180 min after an oral 75-g glucose load; ΣPG, sum of the plasma insulin levels before and 30, 60, 90, 120, and 180 min after an oral 75-g glucose load; ΣIRI/ΣPG, value of ΣIRI divided by ΣPG.

1.88 ± 0.12 l at baseline to 1.50 ± 0.10 l at the end of the second month).

In patient 4, measurements of tissue lipid content were performed using magnetic resonance imaging before and after 3 and 10 d and 1, 2, and 4 months of the leptin-replacement therapy. At baseline, lipid content in her liver was clearly increased (29.0%), whereas that in her skeletal muscle was not increased (4.3%). After the leptin-replacement therapy, a distinct change of lipid content in the liver was not detected at 3 and 10 d (31.5 and 28.4%, respectively), but a substantial and gradual decrease was detected at 1 month and again at 2 and 4 months (23.5, 17.5, and 9.6%, respectively). On the other hand, in the skeletal muscle, no distinct change of lipid content was detected even at 4 months (4.2%).

Metabolic controls after discharge for 8 months

After the initial 4 months of hospitalization, the patients were continuously followed as outpatients on the protocol of twice-daily injection. Their fasting glucose levels (Fig. 2A), HbA1c levels (Fig. 2B), glucose infusion rates during the hyperinsulinemic-euglycemic clamp study (Fig. 2C), triglyceride levels (Fig. 2D), total cholesterol levels (Fig. 2E), and liver volumes (Fig. 2F) at 8 and 12 months were almost unchanged when compared with those at 4 months, the end of the hospitalization.

Once-daily leptin injection

After 12 months of twice-daily leptin injection, the treatment protocol was altered to once-daily dosing without change of total daily dose in patient 1–4. The alteration of leptin injection protocol did not affect the plasma glucose levels before breakfast, lunch, and dinner in four patients (Fig. 3, A–C). Consistent with these results, HbA1c (Fig. 2B) levels and results of the 75-g oral glucose tolerance test (data not shown) in these patients did not change after the protocol alteration. Likewise, glucose infusion rates during the hyperinsulinemic-euglycemic clamp study, triglyceride levels, total cholesterol levels, and liver volumes were unchanged after the alteration of the treatment protocol (Fig. 2, C–F).

Long-term effects

The duration of leptin-replacement therapy was 36 months for patients 1 and 2, 24 months for patient 3, and 18 months for patient 4. The fasting plasma glucose levels and HbA1c levels were well controlled throughout the therapy period (Fig. 2, A and B). The improved glucose infusion rates during the hyperinsulinemic-euglycemic clamp study, decreased triglyceride and total cholesterol levels, and liver volumes after 4 months of leptin-replacement therapy as inpatients

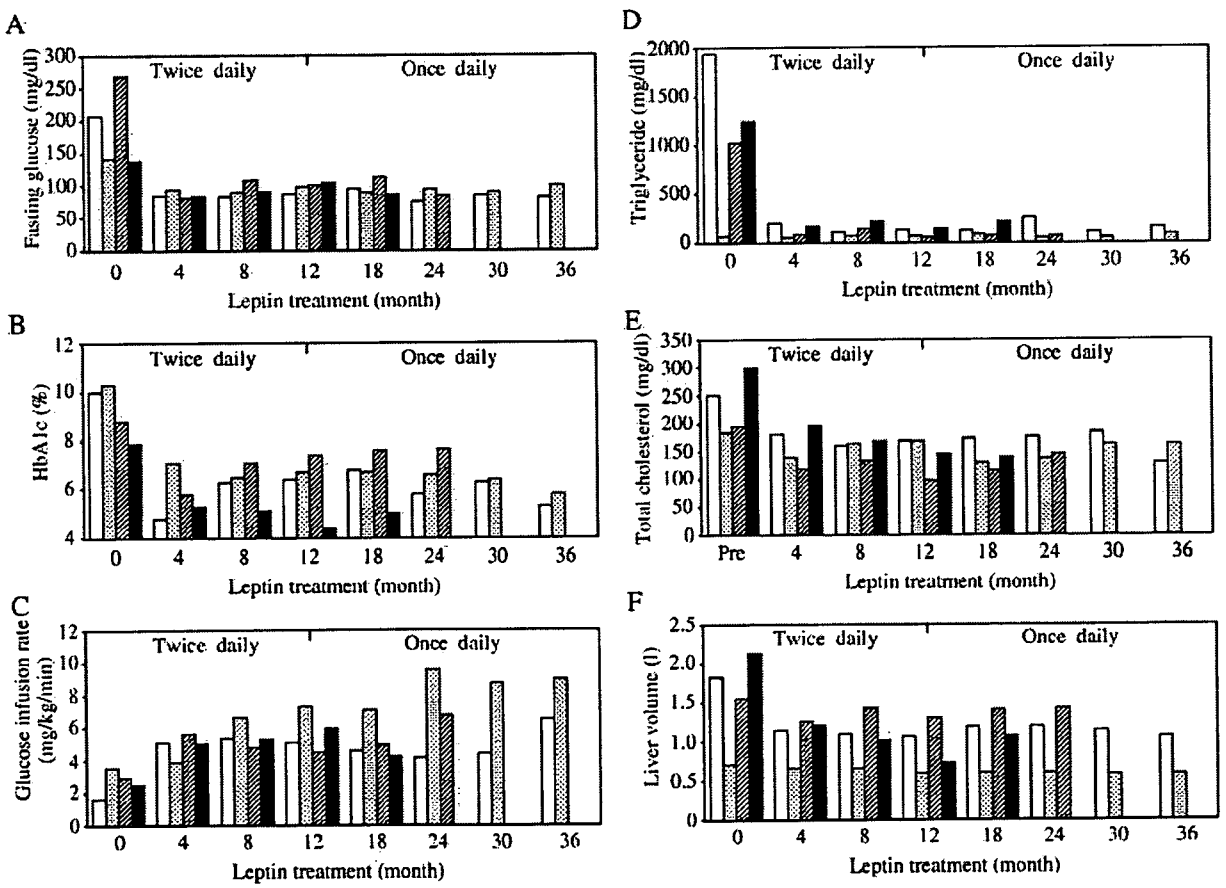

FIG. 2. Fasting plasma glucose levels (A), HbA1c levels (B), glucose infusion rates during the hyperinsulinemic euglycemic clamp study (C), triglyceride levels (D), total cholesterol levels (E), and liver volumes (F) before and after 4, 8, 12, 18, 24, 30, and 36 months of the leptin-replacement therapy in patient 1 (*white bars*), patient 2 (*dotted bars*), patient 3 (*hatched bars*), and patient 4 (*black bars*).

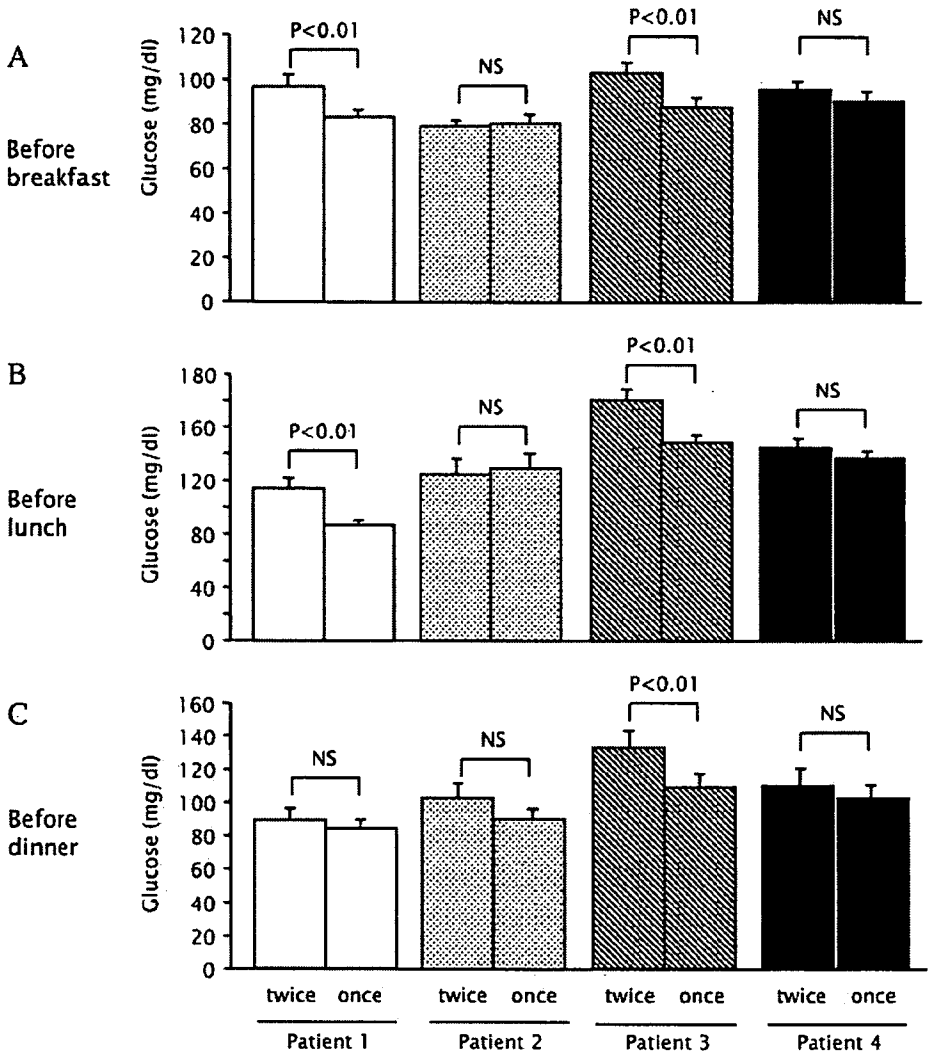

FIG. 3. Comparison of the mean (± SE) plasma glucose levels during the 12th month under the protocol of twice-daily leptin injection and during the 13th month under the protocol of once-daily leptin injection before breakfast (A), lunch (B), and dinner (C) in patient 1 (*white bars*), patient 2 (*dotted bars*), patient 3 (*hatched bars*), and patient 4 (*black bars*). NS, No significance difference ($P > 0.05$) between groups.

were well controlled throughout the therapy period (Fig. 2, C–F).

Antileptin antibodies

Patients 2 and 3, both CGL patients, showed elevations of basal plasma leptin levels, 75.0 and 42.4 ng/ml at the end of the 12th month, respectively. We detected antileptin antibodies in both patients. Antibodies from these patients did not neutralize the action of leptin at all in a bioassay.

Diabetes and other complications

All seven patients had normal renal functions at baseline; however, two patients had microalbuminuria (>30 mg/d), and two patients had macroalbuminuria (>300 mg/d) (Table 1). In addition, five of seven patients had elevated creatinine clearance (mean ± SE, 206.5 ± 22.0 ml/min·1.73 m^2) at the level above 125 ml/min·1.73 m^2. After the initiation of leptin-replacement therapy, urine albumin excretion of patients 1 and 3 with microalbuminuria began to decrease gradually within 1 month and was normalized within 2 months (Fig. 4A). Macroalbuminuria of patients 4 and 6 was also regressed to microalbuminuria within 3 and 1 month, respectively (Fig. 4B). In parallel, the creatinine clearance of the five patients with glomerular hyperfiltration significantly decreased to 129.5 ± 24.5 ml/min·1.73 m^2 (mean ± SE) for the 4-month leptin-replacement therapy ($P < 0.05$). These beneficial effects of leptin on urine albumin excretion and glomerular hyperfiltration were stable for up to 36 months.

Six of seven patients showed no diabetic retinopathy, but patient 7 had a nonproliferative retinopathy at baseline. No deterioration of her retinopathy was observed during the therapy. Six of seven patients had no diabetic neuropathy at baseline, although patient 6 showed neurogenic bladder. During the therapy period, her neurogenic bladder did not worsen, and no patients developed diabetic retinopathy or diabetic neuropathy.

Five of seven patients had moderate to severe acanthosis nigricans at baseline, but the acanthosis nigricans was improved in five patients after the leptin-replacement therapy.

Four of five female patients who were of reproductive age had hypogonadotropic amenorrhea at baseline as previously reported (26, 27) but resumed and sustained normal menses

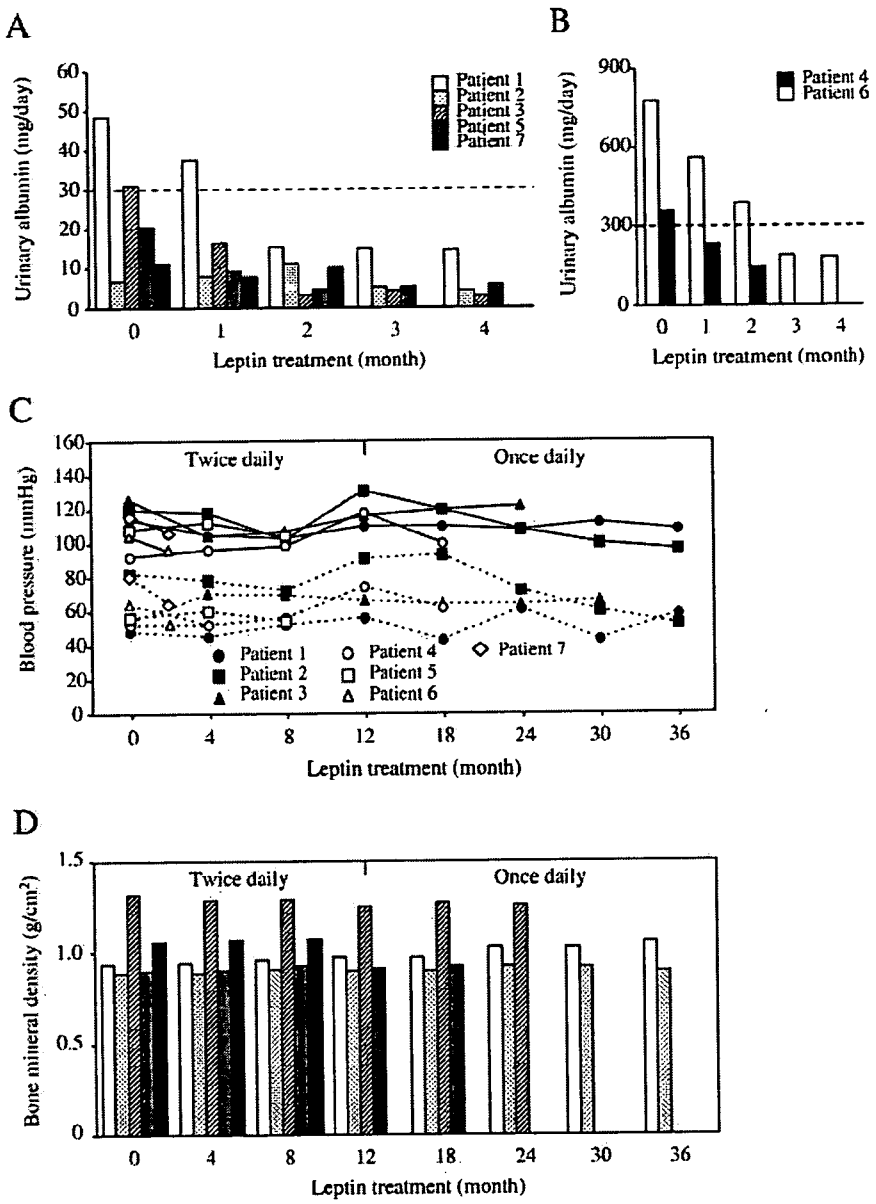

FIG. 4. A and B, Daily excretion levels of urinary albumin before and after 1, 2, 3, and 4 months of the leptin-replacement therapy in patients 1, 2, 3, 5, and 7 and in patients 4 and 6. C, Blood pressure before and after 4, 8, 12, 18, 24, 30, and 36 months of the leptin-replacement therapy in each patient. *Solid lines* indicate systolic blood pressure, and *broken lines* indicate diastolic blood pressure. D, Whole-body bone mineral density before and after 4, 8, 12, 18, 24, 30, and 36 months of the leptin-replacement therapy in patient 1 (*white bars*), patient 2 (*dotted bars*), patient 3 (*hatched bars*), patient 4 (*gray bars*), and patient 5 (*black bars*).

after the initiation of the leptin therapy. In an 11-yr-old girl, the menarche was observed after 12 months of the leptin therapy.

All the patients indicated an improvement in feeling of satisfaction after a meal within 1 or 2 d after the initiation of leptin therapy. This effect was sustained throughout the leptin therapy. For the first 4 months, a tendency of body weight reduction was observed in all the patients, but this change was not significant (mean ± SE, 40.9 ± 3.5 to 38.1 ± 3.1 kg, $P = 0.55$). After the first 4 months, the body weight was almost unchanged throughout the leptin therapy.

Adverse effects

We carefully observed blood pressure in the patients. At baseline, no patients showed hypertension (Table 1), and no distinct elevation of blood pressure was observed at any time throughout the therapy period (Fig. 4C).

No patients showed abnormal bone mineral density (Table 1). Whole-body bone mineral densities of the patients were unchanged for up to 36 months (Fig. 4D).

In all the patients, no other adverse effects of the leptin-replacement therapy including skin reactions at injection sites were detected for up to 36 months.

Discussion

In the present study, all of the leptin injections were done by medical doctors, because self-injection of leptin, which is not approved as a drug, is not permitted in Japan. In addition, all the patients were evaluated as inpatients during the initial 4 months of the leptin-replacement therapy. After leaving the hospital, the patients attended local clinics every day for every leptin injection. This allowed close supervision of leptin-replacement therapy, and the patients' lifestyles including diet and exercise were maintained constant. This

condition could minimize the influences of compliance of leptin injection and changes of diet and exercise. Although we could not include a randomized, placebo-treated control group in the present study because of the rarity and clinical diversity of generalized lipodystrophy, it is highly likely that the improved metabolic control is due to the leptin therapy rather than to an improvement in general compliance associated with participation in the study.

In previous reports, improvements of glucose and triglyceride levels, glucose tolerance, and insulin sensitivity were reported at 1 month (18, 25, 28). The present study clearly shows that significant reductions of fasting glucose levels are achieved within 7 d after the initiation of the leptin-replacement therapy, and substantial reductions of the triglyceride levels are also gained within 7 d (Table 2). These rapid and powerful effects of leptin-replacement therapy were further confirmed with the glucose tolerance test and hyperinsulinemic-euglycemic glucose clamp study performed after 7 or 10 d in patient 4. These rapid effects on glucose and lipid metabolism in the present study are comparable to the rapid effects of leptin administration in two different mouse models of generalized lipodystrophy (16, 17).

After 12 months of the twice-daily leptin treatment, we tried to alter the leptin injection protocol to a once-daily injection without change of total daily dose. This protocol alteration did not affect the controls of glucose and lipid metabolism, and these controls were maintained for up to 24 months (Figs. 2 and 3). These observations demonstrate that a once-daily leptin injection is sufficient to control glucose and lipid metabolism in patients with generalized lipodystrophy.

In the present study, we detected antileptin antibodies in two of four tested patients. Both of them were CGL patients, whereas we did not detect antileptin antibodies in AGL patients. This observation raises the possibility that antileptin antibodies more easily develop in CGL patients than AGL patients. Antibodies from both of our CGL patients did not neutralize the leptin action *in vitro* bioassay. In at least one child with congenital leptin deficiency, the transient appearance of neutralizing antibodies against leptin was reported (21). It is possible to speculate that neutralizing antibodies against leptin more easily develop in patients with congenital leptin deficiency than CGL patients, who have a little leptin levels.

The leptin-replacement therapy substantially ameliorated or did not worsen diabetic complications. Amelioration of proteinuria in the present study is consistent with our and other's previous reports that leptin-replacement therapy significantly alleviates the glomerular injury and proteinuria of lipoatrophic diabetes in mice and humans (29, 30). Although we could not perform renal biopsies, it is highly likely that proteinuria observed in our patients is due to diabetic nephropathy because their proteinuria and hyperfiltration were evidently improved in parallel with the metabolic improvement. These findings indicate that leptin is useful to treat, at least, a certain type of diabetic nephropathy.

The leptin-replacement therapy did not induce elevation of blood pressure in any patients throughout the therapy period (Fig. 4C). We previously demonstrated that a high plasma leptin level that is 10 times of that in normal controls elevates blood pressure through the activation of the sympathetic nervous system in mice (31). It is highly likely that the leptin-replacement therapy at the physiological replacement dose does not affect blood pressure.

Bone mineral density of the patients was within normal range at baseline and was unchanged during the therapy period for up to 36 months (Fig. 4D), consistent with the study reported previously (32). We also previously demonstrated that leptin is a powerful inhibitor of bone formation in mice (33). Although the present study indicates that the leptin-replacement therapy at the physiological replacement dose does not affect bone mineral density in humans, careful follow-up is necessary for young patients.

The effect of leptin on β-cell function remains unclear. Leptin treatment decreased serum insulin levels in mouse models of lipodystrophy (16, 17) and human lipoatrophic patients in the United States (18). These decreases of insulin levels were explained by the reduction of glucose levels rather than the suppressive effect of leptin. Indeed, insulin levels peaked earlier in lipoatrophic patients in the United States, although their overall amounts of insulin secreted in response to the glucose load were less after the leptin therapy than at baseline (28). On the other hand, we here demonstrate that leptin-replacement therapy dramatically improves insulin secretion in Japanese AGL patients. Because glucose-lowering therapy often leads to the restoration of β-cell function in patients with diabetes, this effect can be explained at least in part by the cancellation of glucotoxicity (34). The different responses of insulin secretion to leptin-replacement therapy between AGL and CGL patients could be accounted for by the different duration of diabetes. The impaired insulin responses to the glucose load in CGL patients suggests that their β-cell functions were already exhausted before leptin-replacement therapy. Although whether leptin has an additional effect on β-cell is unknown, we here demonstrate that leptin-replacement therapy is beneficial to the treatment of impaired β-cell function.

The mechanisms through which leptin exerts its insulin-sensitizing actions are unclear at present. Fat accumulation in the insulin target organs, which causes so-called lipotoxicity, is considered to be one of the mechanisms for insulin resistance in patients with lipodystrophy (35). Because in patient 4 with AGL, the improvement of insulin sensitivity was observed before a substantial decrease of tissue lipid content in the liver and muscle, additional studies are necessary to clarify the relationship between insulin resistance and the tissue lipid content in humans.

Based on the effect of the leptin-replacement therapy, it is highly likely that leptin deficiency is the main cause of the metabolic abnormalities associated with lipodystrophy. However, the adipose tissue is recognized as the largest endocrine organ. Therefore, it is possible to speculate that these hormones other than leptin may be involved to some degree in the pathogenesis of lipoatrophic diabetes.

Using leptin-overexpressing transgenic skinny mice (8), we previously reported that leptin treatment is useful for treatment of not only lipoatrophic diabetes mice (17) but also other diabetic mice models (36, 37). These observations along with dramatic effects and safety of the leptin therapy in the

present study indicate possible application of the leptin therapy to diabetes and its complications.

In summary, under strict control of lifestyle and an extremely high compliance of leptin injection, we demonstrate that the leptin-replacement therapy improves both insulin sensitivity and insulin secretion dramatically and rapidly improves glucose and lipid metabolism in patients with generalized lipodystrophy, and its effects are maintained for up to 36 months without any adverse effects. In addition, the leptin-replacement therapy is beneficial to diabetic complications and lipodystrophic ones. The once-daily leptin injection is sufficient to control glucose and lipid metabolism for a long time. It is concluded that leptin-replacement therapy is an effective and safe treatment for long-term improvement of glucose and lipid metabolism and complications in generalized lipodystrophy.

Acknowledgments

We thank Tomoyuki Akashi, Ikuyo Ogawa, and Yasushi Yokokawa (Hamanomachi General Hospital, Fukuoka, Japan); Koichi Kitamura (Kitamura Clinic, Kyoto, Japan); Masanori Adachi and Katsuhiko Tachibana (Kanagawa Children's Medical Center, Kanagawa, Japan); Katsuya Aizu and Hiroshi Mochizuki (Saitama Children's Medical Center, Saitama, Japan); Mari Satoh (Toho University Omori Medical Center, Tokyo, Japan); and Yoichiro Oda (Chigasaki Municipal Hospital, Kanagawa, Japan) for referring the patients originally. We also thank the patients and their families for participating in this study.

Received July 17, 2006. Accepted November 15, 2006.

Address all correspondence and requests for reprints to: Ken Ebihara or Kazuwa Nakao, Department of Medicine and Clinical Science, Kyoto University Graduate School of Medicine, 54 Shogoin Kawahara-cho, Sakyo-ku, Kyoto 606-8507, Japan. E-mail: Kebihara@kuhp.kyoto-u.ac.jp or Nakao@kuhp.kyoto-u.ac.jp.

This work was supported by grants from the Japanese Ministry of Education, Science, Sports, and Culture; the Japanese Ministry of Health, Welfare, and Labor; the Japan Medical Association; Japan Research Foundation for Clinical Pharmacology; the Fujisawa Foundation; the Takeda Science Foundation; and The Study Grant for Japan Insulin Study Group.

Disclosure Statement: K.E., T.K., M.H., H.M., F.M., N.K., T.T., H.C., T.M., T.H., K.H., Y.O., M.F., and K.N. have nothing to disclose. A.M.D. is employed by Amgen Inc.

References

1. Zhang Y, Proenca R, Maffei M, Barone M, Leopold L, Friedman JM 1994 Positional cloning of the mouse obese gene and its human homologue. Nature 372:425–432
2. Frederich RC, Hamann A, Anderson S, Lollmann B, Lowell BB, Flier JS 1995 Leptin levels reflect body lipid content in mice: evidence for diet-induced resistance to leptin action. Nat Med 1:1311–1314
3. Maffei M, Halaas J, Ravussin E, Pratley RE, Lee GH, Zhang Y, Fei H, Kim S, Lallone R, Ranganathan S, Kern PA, Friedman JM 1995 Leptin levels in human and rodent: measurement of plasma leptin and *ob* RNA in obese and weight-reduced subjects. Nat Med 1:1155–1161
4. Considine RV, Sinha MK, Heiman ML, Kriauciunas A, Stephens TW, Nyce MR, Ohannesian JP, Marco CC, McKee LJ, Bauer TL, Caro JF 1996 Serum immunoreactive-leptin concentrations in normal-weight and obese human. N Engl J Med 334:292–295
5. Tartaglia LA, Dembski M, Weng X, Deng N, Culpepper J, Devos R, Richards GJ, Campfield LA, Clark FT, Deeds J, Muir C, Sanker S, Moriarty A, Moore KJ, Smutko JS, Mays GG, Wool EA, Monroe CA, Tepper RI 1995 Identification and expression cloning of a leptin receptor, OB-R. Cell 83:1263–1271
6. Spiegelman BM, Flier JS 1996 Adipogenesis and obesity: rounding out the big picture. Cell 87:377–389
7. Kamohara S, Burcelin R, Halaas JL, Friedman JM, Charron MJ 1997 Acute stimulation of glucose metabolism in mice by leptin treatment. Nature 389: 374–377
8. Ogawa Y, Masuzaki H, Hosoda K, Aizawa-Abe M, Suga J, Suda M, Ebihara K, Iwai H, Matsuoka N, Satoh N, Odaka H, Kasuga H, Fujisawa Y, Inoue G, Nishimura H, Yoshimasa Y, Nakao K 1999 Increased glucose metabolism and insulin sensitivity in transgenic skinny mice overexpressing leptin. Diabetes 48:1822–1829
9. Reitman ML, Arioglu E, Gavrilova O, Taylor SI 2000 Lipodystrophy revisited. Trends Endocrinol Metab 11:410–416
10. Lawrence RD 1946 Lipodystrophy and hepatomegaly with diabetes, lipaemia, and other metabolic disturbances: a case throwing new light on the action of insulin. Lancet 1:724–731, 773–775
11. Rossini AA, Self J, Aoki TT, Goldman RF, Newmark SR, Meguid MM, Soeldner JS, Cahill GF 1977 Metabolic and endocrine studies in a case of lipoatrophic diabetes. Metabolism 26:637–650
12. Shimomura I, Hammer RE, Richardson JA, Ikemoto S, Bashmakov Y, Goldstein JL, Brown MS 1998 Insulin resistance and diabetes mellitus in transgenic mice expressing nuclear SREBP-1c in adipose tissue: model for congenital generalized lipodystrophy. Genes Dev 12:3182–3194
13. Moitra J, Mason MM, Olive M, Krylov D, Gavrilova O, Marcus-Samuels B, Feigenbaum L, Lee E, Aoyama T, Eckhaus M, Reitman ML, Vinson C 1998 Life without white fat: a transgenic mouse. Genes Dev 12:3168–3181
14. Gavrilova O, Marcus-Samuels B, Graham D, Kim JK, Shulman GI, Castle AL, Vinson C, Eckhaus M, Reitman ML 2000 Surgical implantation of adipose tissue reverses diabetes in lipoatrophic mice. J Clin Invest 105:271–278
15. Andreelli F, Hanaire-Broutin H, Laville M, Tauber JP, Riou JP, Thivolet C 2000 Normal reproductive function in leptin-deficient patients with lipodystrophy. J Clin Endocrinol Metab 85:715–719
16. Shimomura I, Hammer RE, Ikemoto S, Brown MS, Goldstein JL 1999 Leptin reverses insulin resistance and diabetes mellitus in mice with congenital lipodystrophy. Nature 401:73–76
17. Ebihara K, Ogawa Y, Masuzaki H, Shintani M, Miyanaga F, Aizawa-Abe M, Hayashi T, Hosoda K, Inoue G, Yoshimasa Y, Gavrilova O, Reitman ML, Nakao K 2001 Transgenic overexpression of leptin rescues insulin resistance and diabetes in a mouse model of lipoatrophic diabetes. Diabetes 50:1440–1448
18. Oral EA, Simha V, Ruiz E, Andewelt A, Premkumar A, Snell P, Wagner AJ, DePaoli AM, Reitman ML, Taylor SI, Gorden P, Garg A 2002 Leptin-replacement therapy for lipodystrophy. N Engl J Med 346:570–578
19. Magre J, Delepine M, Khallouf E, Gedde-Dahl Jr T, Van Maldergem L, Sobel E, Papp J, Meier M, Megarbane A, Bachy A, Verloes A, d'Abronzo FH, Seemanova E, Assan R, Baudic N, Bourut C, Czernichow P, Huet F, Grigorescu F, de Kerdanet M, Lacombe D, Labrune P, Lanza M, Loret H, Matsuda F, Navarro J, Nivelon-Chevalier A, Polak M, Robert JJ, Tric P, Tubiana-Rufi N, Vigouroux C, Weissenbach J, Savasta S, Maassen JA, Trygstad O, Bogalho P, Freitas P, Medina JL, Bonnicci F, Joffe BI, Loyson G, Panz VR, Raal FJ, O'Rahilly S, Stephenson T, Kahn CR, Lathrop M, Capeau J; BSCL Working Group 2001 Identification of the gene altered in Berardinelli-Seip congenital lipodystrophy on chromosome 11q13. Nat Genet 28:365–370
20. Agarwal AK, Arioglu E, De Almeida S, Akkoc N, Taylor SI, Bowcock AM, Barnes RI, Garg A 2002 AGPAT2 is mutated in congenital generalized lipodystrophy linked to chromosome 9q34. Nat Genet 31:21–23
21. Farooqi IS, Matarese G, Lord GM, Keogh JM, Lawrence E, Agwu C, Sanna V, Jebb SA, Perna F, Fontana S, Lechler RI, DePaoli AM, O'Rahilly S 2002 Beneficial effects of leptin on obesity, T cell hyporesponsiveness, and neuroendocrine/metabolic dysfunction of human congenital leptin deficiency. J Clin Invest 110:1093–1103
22. Greenfield MS, Doberne L, Kraemer F, Tobey T, Reaven G 1981 Assessment of insulin resistance with the insulin suppression test and the euglycemic clamp. Diabetes 30:387–392
23. Kawamitsu H, Kaji Y, Ohara T, Sugimura K 2003 Feasibility of quantitative intrahepatic lipid imaging applied to the magnetic resonance dual gradient echo sequence. Magn Reson Med Sci 2:47–50
24. Ebihara K, Kusakabe T, Masuzaki H, Kobayashi N, Tanaka T, Chusho H, Miyanaga F, Miyazawa T, Hayashi T, Hosoda K, Ogawa Y, Nakao K 2004 Gene and phenotype analysis of congenital generalized lipodystrophy in Japan: a novel homozygous nonsense mutation in *seipin* gene. J Clin Endocrinol Metab 89:2360–2364
25. Ebihara K, Masuzaki H, Nakao K 2004 Long-term leptin-replacement therapy for lipoatrophic diabetes. N Engl J Med 351:615–616
26. Oral EA, Ruiz E, Andewelt A, Sebring N, Wagner AJ, DePaoli AM, Gorden P 2002 Effect of leptin replacement therapy on pituitary hormone regulation in patients with severe lipodystrophy. J Clin Endocrinol Metab 87:3110–3117
27. Musso C, Cochran E, Javor E, Young J, DePaoli AM, Gorden P 2005 The long-term effect of recombinant methionyl human leptin therapy on hyperandrogenism and menstrual function in female and pituitary function in male and female hypoleptinemic lipodystrophic patients. Metabolism 54:255–263
28. Javor ED, Cochran EK, Mussa C, Young J, DePaoli AM, Gorden P 2005 Long-term efficacy of leptin replacement therapy in patients with generalized lipodystrophy. Diabetes 54:1994–2002
29. Suganami T, Mukoyama M, Mori K, Yokoi H, Koshikawa M, Sawai K, Hidaka S, Ebihara K, Tanaka T, Sugawara A, Kawachi H, Vinson C, Ogawa Y, Nakao K 2004 Prevention and reversal of renal injury by leptin in a new mouse model of diabetic nephropathy. FASEB J 19:127–129
30. Javor ED, Moran SA, Young JR, Cochran EK, DePaoli AM, Oral EA, Turman MA, Blackett PR, Savage DB, O'Rahilly S, Balow JE, Gorden P 2004 Proteinuric nephropathy in acquired and congenital generalized lipodystrophy:

baseline characteristics and course during recombinant leptin therapy. J Clin Endocrinol Metab 89:3199–3207
31. Maron SA, Patten N, Young JR, Cochran E, Sebring N, Reynolds J, Premkumar A, DePaoli AM, Skarulis MC, Oral EA, Gorden P 2004 Changes in body composition in patients with severe lipodystrophy after leptin replacement therapy. Metabolism 53:513–519
32. Aizawa-Abe M, Ogawa Y, Masuzaki H, Ebihara K, Satoh N, Iwai H, Matsuoka N, Hayashi T, Hosoda K, Inoue G, Yoshimasa Y, Nakao K 2000 Pathophysiological role of leptin in obesity-related hypertension. J Clin Invest 105:1243–1252
33. Elefteriou F, Takeda S, Ebihara K, Magre J, Patano N, Kim CA, Ogawa Y, Liu X, Ware SM, Craigen WJ, Robert JJ, Vinson C, Nakao K, Capeau J, Karsenty G 2004 Plasma leptin level is a regulator of bone mass. Proc Natl Acad Sci USA 101:3258–3263
34. Brownlee M 2003 A radical explanation for glucose-induced β-cell dysfunction. J Clin Invest 112:1788–1790
35. Petersen KF, Oral EA, Dufour S, Befroy D, Ariyan C, Yu C, Cline GW, DePaoli AM, Taylor SI, Gorden P, Shulman GI 2002 Leptin reverses insulin resistance and hepatic steatosis in patients with severe lipodystrophy. J Clin Invest 109:1345–1350
36. Masuzaki H, Ogawa Y, Aizawa-Abe M, Hosoda K, Suga J, Ebihara K, Satoh N, Iwai H, Inoue G, Nishimura H, Yoshimasa Y, Nakao K 1999 Glucose metabolism and insulin sensitivity in transgenic mice overexpressing leptin with lethal yellow agouti mutation: usefulness of leptin for the treatment of obesity-associated diabetes. Diabetes 48:1615–1622
37. Miyanaga F, Ogawa Y, Ebihara K, Hidaka S, Tanaka T, Hayashi S, Masuzaki H, Nakao K 2003 Leptin as an adjunct of insulin therapy in insulin-deficient diabetes. Diabetologia 46:1329–1337

JCEM is published monthly by The Endocrine Society (http://www.endo-society.org), the foremost professional society serving the endocrine community.

Adrenomedullin/Cyclic AMP Pathway Induces Notch Activation and Differentiation of Arterial Endothelial Cells From Vascular Progenitors

Takami Yurugi-Kobayashi, Hiroshi Itoh, Timm Schroeder, Akiko Nakano, Genta Narazaki, Fumiyo Kita, Kentoku Yanagi, Mina Hiraoka-Kanie, Emi Inoue, Toshiaki Ara, Takashi Nagasawa, Ursula Just, Kazuwa Nakao, Shin-Ichi Nishikawa, Jun K. Yamashita

Objective—The acquisition of arterial or venous identity is highlighted in vascular development. Previously, we have reported an embryonic stem (ES) cell differentiation system that exhibits early vascular development using vascular endothelial growth factor (VEGF) receptor-2 (VEGFR2)-positive cells as common vascular progenitors. In this study, we constructively induced differentiation of arterial and venous endothelial cells (ECs) in vitro to elucidate molecular mechanisms of arterial-venous specification.

Methods and Results—ECs were induced from VEGFR2$^+$ progenitor cells with various conditions. VEGF was essential to induce ECs. Addition of 8bromo-cAMP or adrenomedullin (AM), an endogenous ligand-elevating cAMP, enhanced VEGF-induced EC differentiation. Whereas VEGF alone mainly induced venous ECs, 8bromo-cAMP (or AM) with VEGF supported substantial induction of arterial ECs. Stimulation of cAMP pathway induced Notch signal activation in ECs. The arterializing effect of VEGF and cAMP was abolished in recombination recognition sequence binding protein at the Jκ site deficient ES cells lacking Notch signal activation or in ES cells treated with γ-secretase inhibitor. Nevertheless, forced Notch activation by the constitutively active Notch1 alone did not induce arterial ECs.

Conclusions—Adrenomedullin/cAMP is a novel signaling pathway to activate Notch signaling in differentiating ECs. Coordinated signaling of VEGF, Notch, and cAMP is required to induce arterial ECs from vascular progenitors. (*Arterioscler Thromb Vasc Biol.* **2006;26:1977-1984.**)

Key Words: angiogenesis ■ developmental biology ■ embryonic stem cells ■ endothelium ■ vascular biology

Vascular formation is a complicated but well-organized process that involves sprouting, branching, and differential growth of vessels from the primary plexus or existing vessels into a functioning circulation system.[1] During the process, vascular cell specification proceeds in an inseparably coordinated manner.[2] A transmembrane ligand, ephrinB2, and its receptor, the tyrosine kinase EphB4, are reported as molecular markers for arterial and venous endothelial cells (ECs), respectively.[3,4] Recently, various molecular markers specific for arterial ECs have been documented such as Delta-like 4 (Dll4), Bmx, Notch1, Activin receptor-like kinase 1 (Alk1), and others.[5,6] These findings enable the investigation of endothelial specification processes at the cellular and molecular levels being independent of the context of vessel location within the body plan.

The Notch pathway has been highlighted in arterial-venous specification.[7,8] Notch target genes, Hairy and Enhancer-of-split-related basic helix-loop-helix transcription factors, such as grl (gridlock) in zebrafish, or Hey1 and 2 in mammals, are required for arterial vascular development.[9,10] Arterial-venous specification mechanisms in zebrafish were further demonstrated to be a regulatory signaling cascade of sonic hedgehog-vascular endothelial growth factor (VEGF)-Notch-ephrinB2.[5] The molecular machinery for arterial-venous specification in mammals, however, is still undergoing investigation.

See page 1934

cAMP is a ubiquitous second messenger produced in cells and is involved in various biological phenomena including cell growth and differentiation.[11] Nevertheless, little has been reported for the role of cAMP signaling in vascular development. Adrenomedullin (AM) is a multifunctional polypeptide that was originally isolated from human pheochromocytoma.[12] AM exerts its function by increasing the levels of

Original received January 5, 2006; final version accepted May 17, 2006.

From the Laboratory of Stem Cell Differentiation (T.Y.-K., A.N., G.N., F.K., K.Y., M.H.-K., E.I., J.K.Y.), Stem Cell Research Center, Institute for Frontier Medical Sciences, Kyoto University, Japan; Department of Medicine and Clinical Science (T.Y.-K., H.I., K.N.), Kyoto University Graduate School of Medicine, Japan; Institute of Stem Cell Research (T.S.), GSF-National Research Center for Environment and Health, Germany; Department of Medical Systems Control (T.A., T.N.), Institute for Frontier Medical Sciences, Kyoto University, Japan; Institute of Biochemistry (U.J.), University of Kiel, Germany; Laboratory for Stem Cell Biology (S.-I.N.), Center for Developmental Biology, RIKEN, Japan; PRESTO (J.K.Y.), Japan Science and Technology Agency, Japan.

Correspondence to Jun K. Yamashita, Laboratory of Stem Cell Differentiation, Stem Cell Research Center, Institute for Frontier Medical Sciences, Kyoto University, 53 Shogoin Kawahara-cho, Sakyo-ku, Kyoto 606-8507 Japan. E-mail juny@frontier.kyoto-u.ac.jp

Arterioscler Thromb Vasc Biol. is available at http://www.atvbaha.org

DOI: 10.1161/01.ATV.0000234978.10658.41

intracellular cAMP through the binding to its receptor complex, calcitonin receptor-like receptor (CRLR), and receptor activity modifying proteins (RAMP)-2 or RAMP-3.[13] Targeted null mutation of the AM gene shows embryonic lethality[14] with aberrant vascular formation and hemorrhage,[15] or extreme hydrops fetalis and cardiovascular abnormalities, including underdeveloped arterial walls,[16] inferring the significance of AM/cAMP signaling in vascular development.

Pluripotent embryonic stem (ES) cells are potent materials for both regenerative therapeutic approaches and developmental research. We have developed a novel ES cell differentiation system devoid of embryoid body formation or feeder cells that exhibits early vascular development using VEGF receptor-2 (VEGFR2)-positive cells as common progenitors for vascular cells.[17,18] We demonstrated that ES cell-derived VEGFR2$^+$ cells can differentiate into both ECs and mural cells (MCs) (pericytes and vascular smooth muscle cells) and form mature vascular-like structures in vitro.[18] Moreover, transplantation of induced vascular cells can augment the blood flow in tumor angiogenesis.[19] Our ES-derived VEGFR2$^+$ cell differentiation system can recapitulate the vascular development processes and dissect the cellular and molecular mechanisms of each developmental step including endothelial differentiation and specification.

In this study, we aimed to specifically induce arterial and venous ECs and elucidate the mechanisms of arterial-venous specification using our ES cell differentiation system. We successfully induced arterial and venous ECs and demonstrated that the AM/cAMP pathway is another indispensable signaling pathway in EC differentiation and arterial specification in conjunction with VEGF and Notch by reconstructing the arterial EC differentiation process in vitro. Our constructive approach using this ES cell system provides a novel understanding of the cellular and molecular mechanisms of vascular developmental processes.

Methods

Antibodies

Monoclonal antibodies for murine E-cadherin (ECCD2), murine VEGFR2 (AVAS12), and murine VE-cadherin (VECD1) were described previously.[18] Monoclonal antibodies for murine CD31 and CXCR4 were purchased from Pharmingen (San Diego, Calif). MoAb for murine alpha smooth muscle actin (SMA) 1A4 and human estrogen receptor-α (ERα) (F-10) antibody were from Sigma (St Louis, Mo) and Santa Cruz Biotechnology (Santa Cruz, Calif), respectively. Cleaved Notch1 antibody was from Cell Signaling Technology (Beverly, Mass).

Cell Culture

Induction of differentiation of an ES cell line, CCE (gift from Dr Evans), were performed using differentiation medium (alpha minimal essential medium; Gibco, Grand Island, NY) supplemented with 10% fetal calf serum (Equitech-Bio, Kerrville, Tex) and 5×10^{-5} mol/L 2-mercaptoethanol (Gibco) and VEGF165 (R&D System, Minneapolis, Minn) as previously described.[17,18] Other chemicals, rat AM (Peptide Institute. Inc, Osaka, Japan), 8-bromoadenosine-3′:5′-cyclic monophosphate sodium salt (8bromo-cAMP) (Nacalai Tesque, Kyoto, Japan), 8-bromoguanosine-3′:5′-cyclic monophosphate sodium salt (8bromo-cGMP) (Nacalai Tesque), 3-isobutyl-1-methyl-xanthine (IBMX) (Nacalai Tesque), or γ-secretase inhibitor IX, DAPT (Calbiochem, San Diego, Calif), and iloprost (Cayman Chemical, Ann Arbor, Mich) were occasionally added to VEGFR2$^+$ cell culture.

The recombination recognition sequence binding protein at the Jκ site (RBP-J$^{+/+}$), RBP-J$^{+/-}$ and RBP-J$^{-/-}$ D3 ES cell lines have been described previously.[20] The ES cell line NERT$^{\Delta O}$-7[21] was generated by stable introduction of CAG promoter-driven cDNA encoding a fusion protein of a constitutively active part of the intracellular domain of mouse Notch1 and a tamoxifen-sensitive mutant of the hormone binding domain of the human estrogen receptor α (NERT)[22] into EB5 ES cells (gift from Dr Niwa). To induce Notch activation, 4-hydroxytamoxifen (OHT) (50 to 500 nmol/L) (Sigma) was added to NERT$^{\Delta O}$-7 cell-derived VEGFR2$^+$ cells 12 hours after the plating. NERT$^{\Delta O}$-7/Hes-green fluorescent protein (GFP) cells were generated by stable introduction of Hes promoter-driven enhanced GFP (EGFP) gene[23] (gift from Dr Kageyama) into NERT$^{\Delta O}$-7 cells.

Flowcytometry and Cell Sorting

Fluorescence-activated cell sorting (FACS) of ES cells was performed as previously described.[17,18]

Immunocytochemistry

Immunostaining for cultured cells was performed as described.[18,24] Double immunofluorescent staining for CD31 and ERα was performed using anti-ERα antibody (1:50) and anti-CD31 antibody (1:300) as first antibodies, followed by second antibodies, Alexa Fluor 546-conjugated goat anti-rat IgG (1:500) and Alexa Fluor 488-conjugated goat anti-mouse IgG (1:500) (Molecular Probes, Eugene, Ore). For double staining for ephrinB2 and CD31, the fixed culture slides were incubated with EphB4-human immunoglobulin Fc portion chimeric protein (EphB4-Fc) (1:50; R&D system), followed by peroxidase-conjugated goat IgG fraction to human IgG Fc (1:500; ICN Biomedicals, Inc, Aurora, Ohio). TSA Biotin system (Tyramid signal amplification; PerkinElmer Life Science, Boston, Mass) was used for amplification of the signal for EphB4-Fc staining. EphrinB2$^+$ cells were visualized by using streptavidin-Alexa Fluor488-conjugate (Molecular Probes). Phycoerythrin-conjugated anti-CD31 antibody (Pharmingen) and DAPI (Molecular Probes) were added together with streptavidin-conjugated alexa 488. Cleaved intracellular domain of Notch (NICD) staining was performed using TSA Biotin System (PerkinElmer) with cleaved Notch1 antibody (1:300), followed by peroxidase-labeled anti-rabbit IgH (1:250; Vector Laboratories, Burlingame, Calif).

Single-Cell Analysis

Single-cell sorting of VEGFR2$^+$ cells using 96-well dishes was performed as previously described.[18] Colonies were stained for ephrinB2 using EphB4-Fc by TSA kit with streptavidin-conjugated horseradish peroxidase, followed by addition of phycoerythrin-conjugated anti-CD31 antibody and DAPI. Numbers of colonies including CD31$^+$ cells (EC-including), colonies including ephrinB2$^+$ cells (arterial EC-including), and ephrinB2$^+$ arterial EC numbers in each arterial EC-including colonies, as well as the total number of colonies that appeared were counted. 1692 VEGFR2$^+$ cells were cultured with VEGF alone, and 1128 cells were cultured with VEGF and 8bromo-cAMP. Total colony numbers in every 100 sequential wells, EC-including or arterial EC-including colony numbers in every 10 sequential colonies that appeared, and the arterial EC number in each arterial EC-including colony were statistically evaluated.

Measurement of Intracellular cAMP

After 3 days culture of VEGFR2$^+$ cells (2 to 10×10^5 cells), cells were harvested and counted. Intracellular cAMP concentration in total harvested cells was evaluated using cAMP Biotrak Enzyme Immunoassay system kit (Amersham Bioscience). Concentration was normalized by cell number.

In Situ Hybridization

In situ hybridization for CXCR4 was performed as previously described.[25]

Reverse-Transcription Polymerase Chain Reaction Amplification

Total RNA was isolated from sorted VE-cadherin$^+$ ECs induced by VEGF alone, or 8bromo-cAMP and VEGF treatment, using ISOGEN (Nippon Gene, Toyama, Japan). The reverse-transcription polymerase chain reaction was performed as described[24] using indicated primers (supplemental Table I, available online at http://atvb.ahajournals.org).

Statistical Analysis

Statistical analysis of the data was performed using Student t test. $P<0.05$ was considered significant.

Results

We first examined the effects of AM and cAMP on EC differentiation from ES cell-derived VEGFR2$^+$ progenitor cells. VEGFR2$^+$ cells were sorted by FACS and re-cultured for 3 days on type IV collagen-coated dishes in differentiation medium (see Methods) with VEGF (50 ng/mL) and other factors. Double immunostaining of induced cells with an EC marker, CD31, and a MC marker, SMA, revealed that VEGF treatment selectively induced both CD31$^+$ ECs and SMA$^+$ MCs from VEGFR2$^+$ cells as previously reported[18] (Figure 1A). Simultaneous stimulation of cAMP signaling in the presence of VEGF substantially enhanced EC induction from VEGFR2$^+$ cells (Figure 1B to 1D). VEGF together with 0.5 mmol/L 8bromo-cAMP resulted in substantial induction of ECs (Figure 1D), whereas 8bromo-cAMP treatment alone exerted almost no effect (data not shown). Another cyclic monophosphate analog, 8bromo-cGMP, showed no effect on VEGF-induced EC induction (data not shown). Addition of 10^{-6}mol/L AM also enhanced VEGF-stimulated EC induction, but to a lesser extent than 8bromo-cAMP (Figure 1B). Enhancement of the effect of AM by the simultaneous administration of a phosphodiesterase inhibitor, IBMX, revealed comparable EC induction with 8bromo-cAMP (Figure 1C). We quantitatively evaluated the EC-inducing effects of AM and 8bromo-cAMP using flow cytometry. VEGF treatment induced ECs to ≈30% of total cells. AM increased VEGF-induced ECs up to ≈50%. AM with IBMX or 8bromo-cAMP showed efficient induction of ECs to ≈70% of total cells (Figure 1E). Intracellular concentration of cAMP in the differentiating cells was significantly increased by AM with VEGF (667.6 fmol±215.1/10^6 cells; n=6; $P<0.01$ versus VEGF alone), or AM and IBMX with VEGF (1142 fmol±270.1/10^6 cells; n=6; $P<0.001$ versus VEGF alone) than that with VEGF alone (372.2 fmol±58.5/10^6 cells; n=6), and was comparable or lower level with those observed in previous reports using human umbilical vein ECs.[26] These results indicated that the AM/cAMP pathway specifically and synergistically enhances the effect of VEGF on EC differentiation from VEGFR2$^+$ progenitor cells.

Next, we investigated the features of induced ECs with AM/cAMP treatment with regard to arterial-venous diversity. Arterial ECs were evaluated by ephrinB2 expression, an arterial EC marker, detected by the binding of EphB4-Fc.[27]

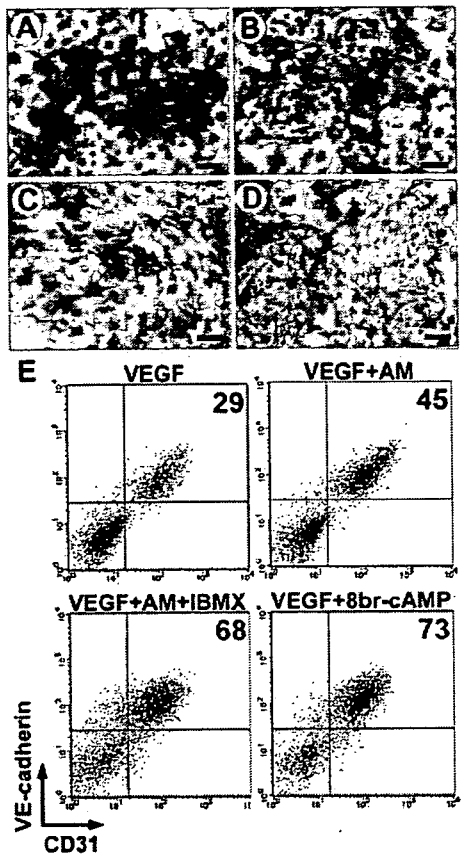

Figure 1. The effect of AM and cAMP on EC induction from VEGFR2$^+$ cells. A to D, Double immunostaining of induced ECs and MCs with an EC marker CD31 (purple) and MC marker SMA (brown) after 3 days of culture of VEGFR2$^+$ cells on type IV collagen-coated dishes in various conditions. A, VEGF treatment alone (50 ng/mL). CD31$^+$ EC sheets and SMA$^+$ MCs appear. B, VEGF with 10^{-6} mol/L AM. A slight increase of ECs is observed. C, VEGF with 10^{-6} mol/L AM and 10^{-4} mol/L IBMX. D, VEGF with 0.5 mmol/L 8bromo-cAMP. Remarkable EC induction occurs. Scale bars: 100 μm. E, Flow cytometry of induced cells from VEGFR2$^+$ cells with endothelial markers VE-cadhein and CD31. Left upper panel, VEGF treatment alone (50 ng/mL). Right upper panel, VEGF with 10^{-6} mol/L AM. Left lower panel, VEGF with 10^{-6} mol/L AM and 10^{-4} mol/L IBMX. Right lower panel, VEGF with 0.5 mmol/L 8bromo-cAMP. Percentages of VE-cadherin$^+$/CD31$^+$ ECs of total VEGFR2$^+$ cell-derived cells are indicated.

We double-immunostained ECs using anti-CD31 antibody and EphB4-Fc (Figure 2A to 2D). With VEGF treatment alone, very few ephrinB2$^+$ arterial ECs were observed among the ECs that appeared, indicating that venous ECs were mainly induced in this condition (Figure 2A). Surprisingly, remarkable appearance of ephrinB2$^+$ ECs was clearly observed by the stimulation of cAMP pathway. That is, addition of AM induced ephrinB2$^+$ EC appearance (Figure 2B). AM with IBMX, or 8bromo-cAMP together with VEGF, showed substantial induction of ephrinB2$^+$ ECs (Figure 2C and 2D). Messenger RNA expression of arterial EC markers, ephrinB2, Dll4, Notch1, Notch4, Alk1, and neuropilin1 (NRP1) were increased in 8bromo-cAMP and VEGF-treated ECs (Figure 2E). In contrast, venous EC markers, COUP-TFII transcription factor[28] and NRP2[29] mRNA were decreased by

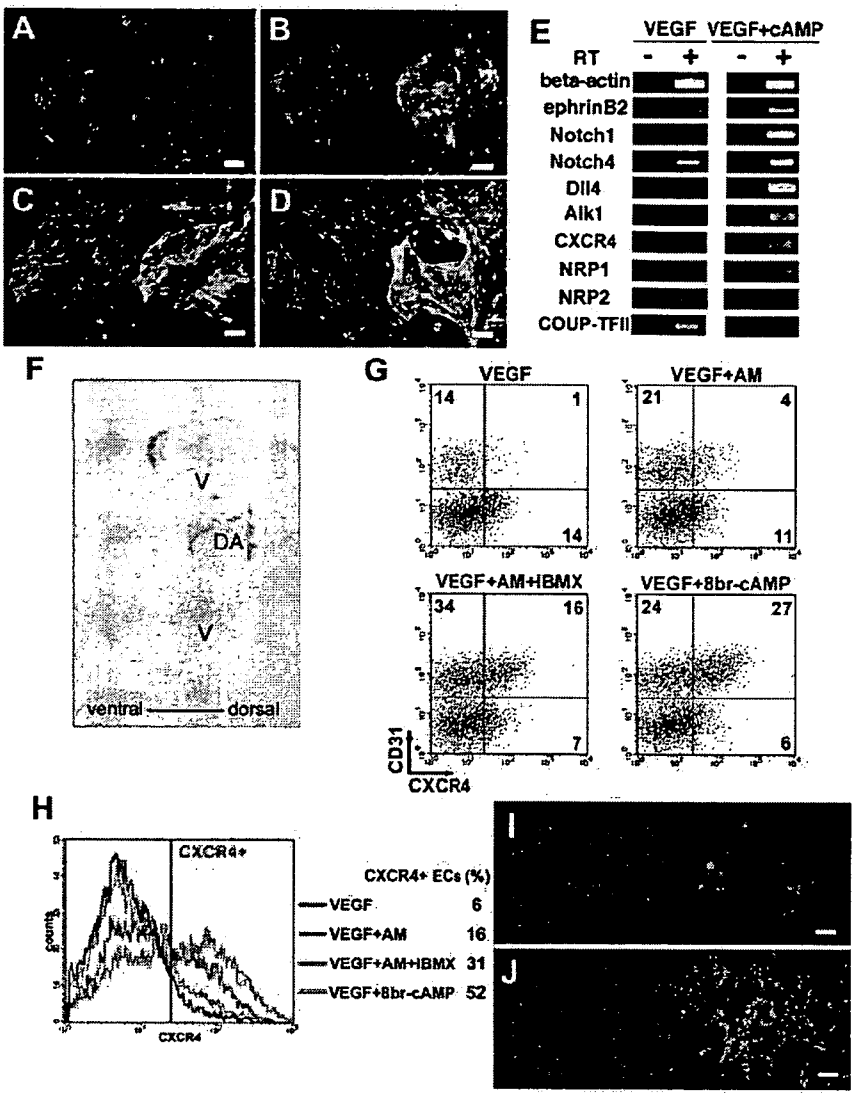

Figure 2. The effect of AM and cAMP on arterial EC induction from VEGFR2$^+$ cells. A to D, Double fluorescent staining for CD31 and ephrinB2 after 3 days of culture of VEGFR2$^+$ cells. Left panels, CD31 (pan-ECs, red) and DAPI (blue). Right panels, EphB4-Fc (ephrinB2$^+$ arterial ECs, green) and DAPI (blue). A, VEGF treatment alone (50 ng/mL). B, VEGF with 10^{-6} mol/L AM. C, VEGF with 10^{-6} mol/L AM and 10^{-4} mol/L IBMX. D, VEGF with 0.5 mmol/L 8bromo-cAMP. Scale bars: 100 μm. E, Reverse-transcription polymerase chain reaction showing mRNA expression of arterial markers (ephrinB2, Notch1, Notch4, Dll4, Alk1, CXCR4, and NRP1) and venous marker (NRP2 and COUP-TFII) in purified ECs induced by VEGF treatment alone or VEGF and 8bromo-cAMP treatment. F, Aortic EC-specific expression of CXCR4 (purple) by in situ hybridization of the isolated aorta-gonad-mesonephros (AGM) region in E11.5 mouse embryo. DA indicates dorsal aorta; V, Cardinal veins. G, Flow cytometry for CD31 and CXCR4 expression. Left upper panel, VEGF treatment alone (50 ng/mL). Right upper panel, VEGF with 10^{-6} mol/L AM. Left lower panel, VEGF with 10^{-6} mol/L AM and 10^{-4} mol/L IBMX. Right lower panel, VEGF with 0.5 mmol/L 8bromo-cAMP. H, Expression profile of CXCR4 in CD31$^+$ ECs by flowcytometry. VEGF treatment alone (blue line), VEGF with 10^{-6} mol/L AM (green line), VEGF with 10^{-6} mol/L AM and 10^{-4} mol/L IBMX (red line), and VEGF with 0.5mmol/L 8bromo-cAMP (orange line) are shown. Percentages of CXCR4$^+$ arterial ECs in total ECs are indicated. I and J, Gross appearance of ephrinB2$^+$ arterial EC induction from VEGFR2$^+$ cells (plated at 2×10^4 cells/cm^2). Left panels, DAPI (blue). Right panels, EphB4-Fc (ephrinB2$^+$ arterial ECs, green). I, VEGF treatment alone (50 ng/mL). J, VEGF with 0.5 mmol/L 8bromo-cAMP. Increase in cell number (DAPI) and substantial arterial EC induction were observed. Scale bars: 400 μm.

8bromo-cAMP and VEGF treatment (Figure 2E). These results indicated that stimulation of cAMP pathway induces arterial ECs.

We further attempted to quantitatively evaluate arterial EC induction at the cellular level. CXCR4, a 7-transmembrane G-protein-coupled receptor, is the receptor of CXCL12 (also known as stromal cell-derived factor-1). Recently, CXCR4 has been reported to be expressed in ECs in the superior mesenteric artery, but not in the superior mesenteric vein, and involved in the formation of arteries in the gastrointestinal tract.[25,30] We examined CXCR4 expression in the mouse embryo by in situ hybridization and found that CXCR4 was detected in ECs of the dorsal aorta but not of cardinal veins in aorta-gonado-mesonephros (AGM) region of E11.5 embryos (Figure 2F). In addition, mRNA expression of CXCR4 was increased in 8bromo-cAMP and VEGF-treated ECs together with other arterial EC markers (Figure 2E), indicating that CXCR4 is another arterial EC marker. FACS analysis using an anti-CXCR4 antibody successfully quantified arterial EC induction by AM or 8bromo-cAMP treatment. Most of ECs induced by VEGF treatment alone (>90% to 95%) were negative for CXCR4. CXCR4$^+$/CD31$^+$ arterial ECs were induced in the presence of AM together with VEGF. Addition of AM with IBMX, or 8bromo-cAMP further increased CXCR4$^+$/CD31$^+$ arterial EC appearance (Figure 2G). Overall, 8bromo-cAMP and VEGF treatment induced ≈5- to 10-fold more CXCR4$^+$ arterial ECs compared with VEGF treatment alone. AM with VEGF treatment showed slight effect on the arterial EC induction. Simultaneous administration of AM and IBMX with VEGF enhanced the arterializing effect of AM (Figure 2H). These results indicated that cAMP signaling mainly contributes to the arterial EC induction. The maximum percentage of arterial ECs within total ECs was increased to ≈60% by 8bromo-cAMP and VEGF (Figure 3F). Addition of 8bromo-cAMP with VEGF led to an increase in total cell number, total EC number, and arterial EC percentage, resulting in ≈70-times increment of induced arterial EC number than those by VEGF alone (Figure 2I and 2J). Higher doses of VEGF (100 to 200 ng/mL) alone or 8bromo-cGMP (0.5 mmol/L) with VEGF

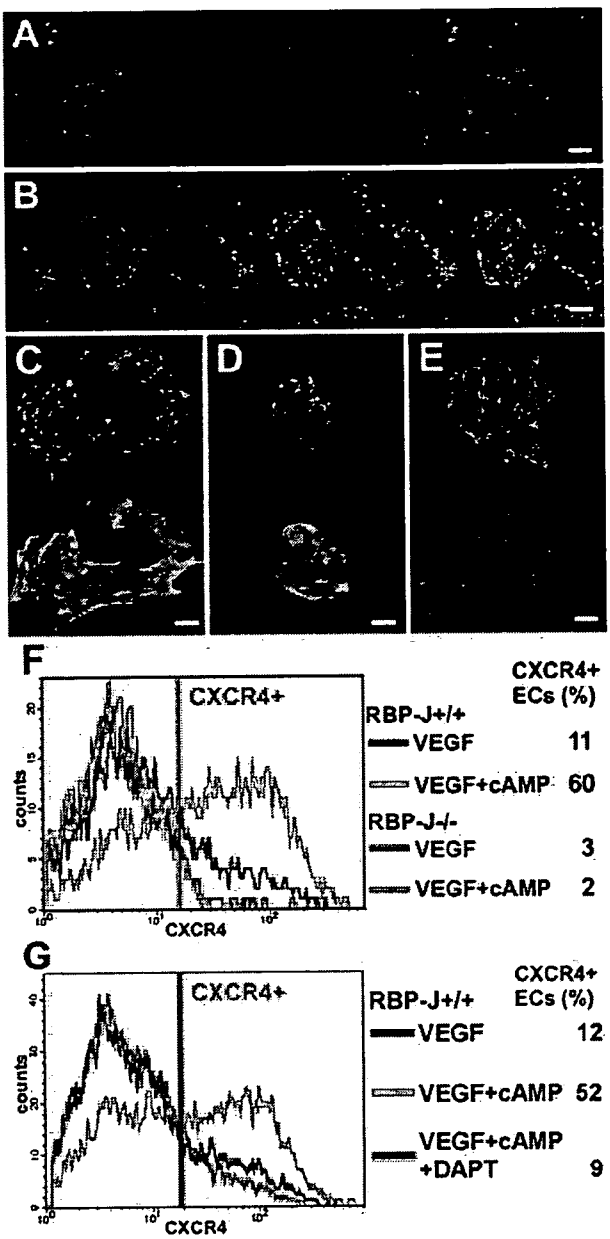

Figure 3. Essential role of Notch signaling in arterial EC induction. A and B, Double fluorescent staining of cleaved Notch intracellular domain (NICD) and CD31 for induced ECs. Left panels, CD31 (pan-ECs, red). Middle panels, Cleaved NICD (green). Right panels, Merged image. A, VEGF treatment alone (50 ng/mL). B, VEGF with 0.5 mmol/L 8bromo-cAMP. Scale Bars: 200 μm. C to E, Double-fluorescent staining of CD31 and ephrinB2 for ECs induced by VEGF with 8bromo-cAMP using RBP-J–deficient ES cells. Upper panels, CD31 (pan-ECs, red) and DAPI (blue). Lower panels, EphB4-Fc (ephrinB2$^+$ arterial ECs, green) and DAPI (blue). C, RBP-J$^{+/+}$ ES cells. D, RBP-J$^{+/-}$ ES cells. E, RBP-J$^{-/-}$ ES cells. Scale bars: 100 μm. F and G, Expression profile of CXCR4 in CD31$^+$ ECs. F, Blue and green lines: RBP-J$^{+/+}$ cells. VEGF treatment alone (blue line), VEGF with 0.5 mmol/L 8bromo-cAMP (green line). Red and orange lines: RBP-J$^{-/-}$ cells. VEGF alone (red line), VEGF with 0.5 mmol/L 8bromo-cAMP (orange line). Percentages of CXCR4$^+$ arterial ECs in total ECs are indicated. G, RBP-J$^{+/+}$ cells. VEGF treatment alone (blue line), VEGF with 0.5 mmol/L 8bromo-cAMP (green line). VEGF with 8bromo-cAMP and 2.5 μmol/L DAPT (red line).

Single-Cell Analysis of VEGFR2$^+$ Cell Culture

	VEGF Alone	VEGF With 8bromo-cAMP
Total colony, n (per every 100 sequential wells)	5.62±1.74 (n=16)	16.0±6.06 (n=11)*
EC-including colony, n (per every 10 sequential colonies)	3.40±2.20 (n=15)	7.00±1.70 (n=19)*
AEC-including colony, n (per every 10 sequential colonies)	1.27±1.10 (n=15)	3.63±1.30 (n=19)*
AEC number (per each AEC-including colony)	1.69±0.87 (n=16)	4.51±2.77 (n=76)*

*$P<0.01$ vs VEGF alone.
AEC indicates arterial endothelial cell; EC, endothelial cell.

treatment did not show arterial EC induction. Administration of iloprost (10^{-7} to 10^{-5} mol/L), an analogue of prostaglandin-I2 that elevates intracellular cAMP in mature ECs, showed almost no arterial inducing effect even with VEGF treatment (data not shown). These results indicated that AM/cAMP signaling is a novel potent and specific inducer of arterial ECs from vascular progenitor cells.

To further evaluate the mechanism of AM/cAMP-stimulated arterial EC induction, we performed single-cell culture of VEGFR2$^+$ cells. Colonies obtained from single VEGFR2$^+$ cells were counted and evaluated by staining for CD31, ephrinB2, and DAPI (Table). VEGF and 8bromo-cAMP treatment significantly increased the total number of colonies that appeared, number of EC-including colonies, and arterial EC-including colonies in appeared colonies, and arterial EC numbers in each arterial EC-including colony than VEGF alone. These results suggest that cAMP increased survival of VEGFR2$^+$ progenitor cells, differentiation of ECs and arterial ECs from progenitor cells that survived, and proliferation of arterial ECs. cAMP, thus, should be involved in multi steps of arterial EC differentiation processes.

We then examined the role of Notch signaling in arterial EC induction in this system. Activation of Notch on ligand binding is accompanied by proteolytic processing that releases intracellular domain of Notch (NICD) from the membrane. The NICD then translocates into the nucleus and associates with RBP-J, a DNA-binding protein, to form a transcriptional activator, which turns on transcription of a set of target genes.[31] First, we examined Notch activation by cAMP treatment with immunostaining of cleaved NICD. Whereas Notch signal was not activated in most of ECs induced by VEGF alone (Figure 3A), administration of 8bromo-cAMP together with VEGF clearly induced nuclear localization of cleaved NICD in ECs, indicating that stimulation of cAMP pathway can activate Notch signaling in differentiating ECs (Figure 3B). cAMP is, thus, found to be a novel signaling pathway that interacts with and activates Notch signaling in EC lineages. Then, we performed a loss-of-function study using RBP-J–deficient ES cells that lack Notch signaling activation.[20] VEGFR2$^+$ cells derived

from RBP-J$^{+/+}$, RBP-J$^{+/-}$, or RBP-J$^{-/-}$ ES cells were sorted and re-cultured with VEGF in the presence of 8bromo-cAMP. Arterial EC induction observed in RBP-J$^{+/+}$ (Figure 3C) or RBP-J$^{+/-}$ ES cells (Figure 3D) was completely abolished in RBP-J$^{-/-}$ ES cells (Figure 3E). FACS analysis using CXCR4 further demonstrated that induction of CXCR4^{+} arterial ECs observed in RBP-J$^{+/+}$ was completely abolished in RBP-J$^{-/-}$ ES cells (Figure 3F). Similarly, administration of γ-secretase inhibitor, DAPT (2.5μmol/L), which inhibits proteolytic processing of Notch to activate its signaling, to VEGFR2^{+} cell culture also completely blocked the arterial EC induction (Figure 3G). These results indicate that Notch signaling is essential for arterial EC induction in this ES cell system, and correlates with previous reports in zebrafish[32,33] and mouse[34,35] genetic animal models.

Next, we examined the effect of a gain-of-function of Notch in arterial EC induction. We used an ES cell line NERT$^{\Delta OP}$-7,[21] in which signaling of the activated intracellular domain of murine Notch1 can be regulated using an OHT-inducible system.[22] NERT$^{\Delta OP}$-7 ES cell-derived VEGFR2^{+} cells were sorted and re-cultured with VEGF in the presence or absence of OHT. In the absence of OHT, NERT protein was located mainly in the cytoplasm of induced CD31^{+} ECs and other cell types (supplemental Figure IA, available online at http://atvb.ahajournals.org). After addition of OHT, NERT protein translocated to the nucleus (supplemental Figure IB). Notch signal activation in VEGF-induced ECs was evaluated by FACS using NERT$^{\Delta OP}$-7/Hes-GFP cells carrying HES promoter-driven GFP gene (supplemental Figure IC). Addition of 8bromo-cAMP induced endogenous Notch activation in ECs, correlating with our previous results shown in Figure 3A and 3B. OHT treatment showed stronger Notch signal activation through NERT protein than 8bromo-cAMP treatment. Simultaneous stimulation by 8bromo-cAMP and OHT additionally enhanced Notch activation in induced ECs. These results indicate that NERT$^{\Delta OP}$-7 cell system can successfully induce Notch signal activation in differentiating ES cells. NERT$^{\Delta OP}$-7 cell-derived ECs induced by VEGF alone were negative for ephrinB2 (Figure 4A). Unexpectedly, hardly any arterial ECs appeared after Notch activation with OHT, even when co-stimulated with VEGF (Figure 4B). Although ephrin-B2^{+} arterial ECs were successfully induced by VEGF with 8bromo-cAMP (Figure 4C), no apparent effect of OHT was observed on the cAMP-stimulated arterial EC induction with ephrinB2 staining (Figure 4D). FACS analysis further demonstrated that activation of Notch signaling by OHT failed to induce CXCR4^{+} arterial ECs and, moreover, activation of Notch signaling with OHT did not affect, or often reduced, cAMP-induced CXCR4^{+} arterial EC induction (Figure 4E). These results indicate that Notch signal is not sufficient or at least aberrant activation of Notch is not beneficial, for arterial EC induction. This is compatible with the previous in vivo study using activated Notch4-transgenic mice in that activation of Notch signaling in embryonic endothelium led to disorganized vascular networks but did not document arterial induction.[36]

Taken together, VEGF appears essential for EC differentiation from VEGFR2^{+} cells, and venous ECs can be induced by VEGF alone. For arterial EC induction, however, VEGF

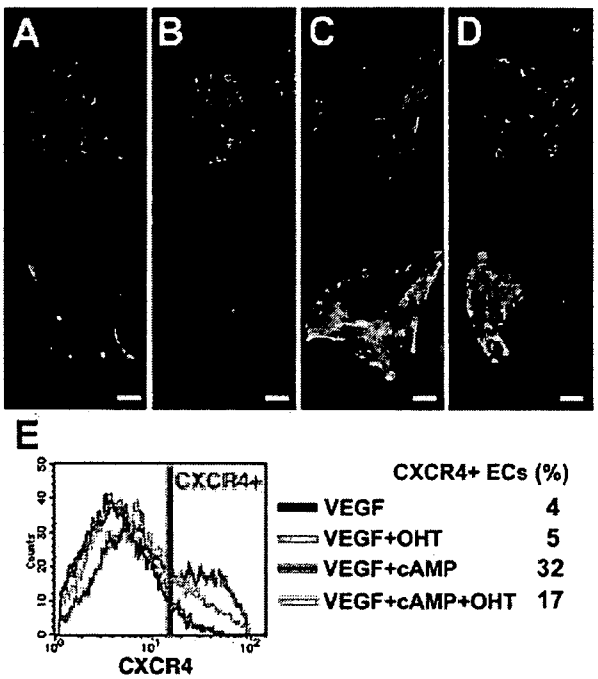

Figure 4. Effects of activated Notch on arterial EC induction from VEGFR2^{+} cells. A-D, Double-fluorescent staining of CD31 and ephrinB2 for induced ECs using NERT$^{\Delta OP}$-7 ES cells. Upper panels, CD31 (pan-ECs, red) and DAPI (blue). Lower panels, EphB4-Fc (ephrinB2^{+} arterial ECs, green) and DAPI (blue). A, VEGF treatment alone (50 ng/mL). B, VEGF and 150 nmol/L OHT. C, VEGF and 0.5 mmol/L 8bromo-cAMP. D, VEGF, 0.5mmol/L 8bromo-cAMP, and 150 nmol/L OHT. Scale bars: 100 μm. E, Expression profile of CXCR4 in CD31^{+} ECs. VEGF alone (blue line), VEGF and OHT (green line), VEGF and 8bromo-cAMP (red line), and VEGF, 8bromo-cAMP, and OHT (orange line) are shown. Percentages of CXCR4^{+} arterial ECs in total ECs are indicated.

and Notch signaling is essential but not sufficient. AM/cAMP pathway can activate Notch signaling, and is another important signaling to induce arterial ECs. Coordinated signaling of VEGF, Notch, and cAMP is the combination that composes a sufficient condition to constructively induce arterial ECs from vascular progenitor cells.

Discussion

Our findings provide the first demonstration to our knowledge of arterial and venous EC induction from ES cells by constructively reproducing endothelial differentiation processes in vitro. Here we showed that cAMP and AM play specific roles in EC differentiation, especially for arterial EC induction, from VEGFR2^{+} vascular progenitors. We have shown that AM enhances proliferation and migration of cultured ECs and can promote angiogenesis in gel plug assays in vivo.[37] Recently, AM was reported to enhance angiogenic potency of bone marrow cell transplantation.[38] AM should be a novel potent candidate for an endogenous ligand for EC differentiation as well as arterial EC induction.

Our results showed that stimulation of cAMP pathway can activate Notch signaling in EC lineage. To date, little evidence of Notch activation by cAMP pathway has been reported. In neuronal cells, cAMP-response element-binding protein increased expression of presenilin-1, a component of

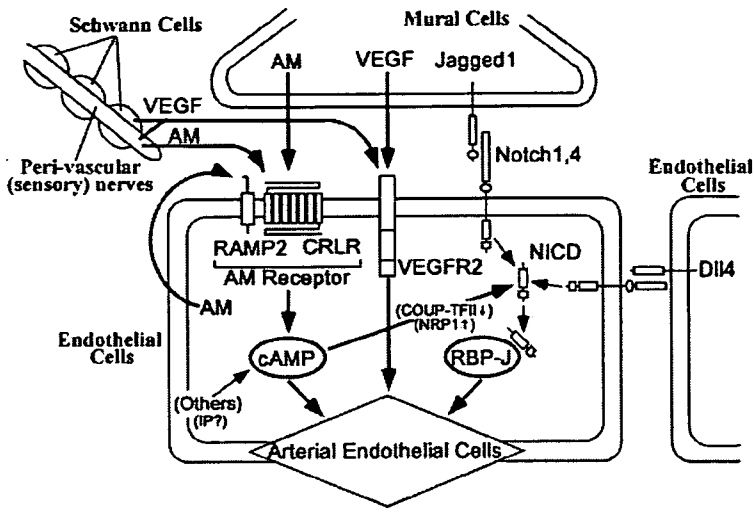

Figure 5. Cellular and molecular mechanisms of arterial EC induction. Putative autocrine/paracrine system for arterial induction in vascular wall. Signals for arterial induction, VEGF, Notch, and AM/cAMP components exist in the vascular wall. VEGFR2, AM receptor complex, RAMP2 and CRLR, and Notch1 and 4 are expressed in ECs. However, their ligands, VEGF, AM, and Jagged1 are expressed in mural cells (MCs). Moreover, AM is expressed in ECs and perivascular nerves. VEGF is produced from peripheral sensory nerves and Schwann cells. Notch ligands, Dll4, and Jagged1 are expressed in arterial ECs. These autocrine/paracrine signals among ECs, MCs, and other perivascular tissues should coordinately regulate the arterial induction and maintenance.

γ-secretase, through transcriptional activation.[39] A similar mechanism may contribute in EC and EC progenitors to induce Notch activation. Recently, COUP-TFII has been reported to repress Notch signaling through suppressing NRP1 expression to maintain vein identity.[28] Administration of 8bromo-cAMP did not increase mRNA expression of Notch ligands (ie, jagged1, 2, Delata-like1, 3, 4) in surrounding mural cells (data not shown), but suppressed COUP-TFII and increased NRP1 expression in ECs. These results suggest that cAMP pathway may activate Notch signaling through the suppression of COUP-TFII expression. cAMP pathway, thus, may regulate the determination of cell fates between arterial and venous ECs. Although Dll4 and Notch signaling were reported to be growth-suppressive on mature ECs through downregulation of VEGFR2 and NRP1 expression,[40] forced Notch activation with OHT did not affect on VEGFR2 and NRP1 mRNA expression in differentiating ECs (data not shown). Notch signaling may possess differentiation stage-specific roles in EC differentiation and proliferation. Precise molecular interactions among these pathways should be further investigated to figure out the whole scheme of arterial-venous specification.

In the vascular wall, VEGFR2, Notch1 and 4, and AM receptor complex, CRLR, RAMP-2 and -3, are expressed in ECs.[5,6] On the other hand, their ligands, VEGF, Jagged1, and AM, are expressed in MCs.[8,41,42] Dll4 and AM are also expressed in ECs. We confirmed AM mRNA expression in ES cell-derived ECs and MCs, and RAMP-2 and CRLR mRNA in ECs by reverse-transcription polymerase chain reaction analysis. Low-level expression of prostaglandin-I2 receptor mRNA was also observed in ECs (data not shown). Moreover, peripheral sensory nerve and Schwann cell-derived VEGF are reported to be involved in arterial EC induction.[43] AM is demonstrated to be expressed in perivascular nerves in the rat mesenteric artery.[44] The autocrine/paracrine cross-talk of VEGF, Notch, and AM/cAMP signaling between ECs and MCs, and signals from other perivascular tissues, should coordinately regulate vascular development including the induction and maintenance of the arterial structures (Figure 5). Combinatory signaling of VEGF, Notch, and cAMP may mimic these arterial-inducing machineries in vivo to achieve constructive induction of arterial ECs from vascular progenitor cells in vitro.

Our constructive approach has successfully provided a novel understanding for the mechanisms of arterial EC differentiation. This study, thus, would provide a potent novel strategy as constructive developmental biology to dissect cell differentiation processes and contribute to regenerative medicine.

Acknowledgments

We thank Dr Ohtsuka and Dr Kagayama for Hes promoter gene constructs. We also thank Drs Takahashi and Hoshino for critical reading of the manuscript.

Sources of Funding

J.K.Y. is supported by grants from the Ministry of Education, Science, Sports, and Culture of Japan, the Ministry of Health, Labor, and Welfare of Japan, and PRESTO JST. U.J. is supported by the Deutsche Forschungsgemeinschaft Priority Program 1109 "Stem Cells" and Sonderforschungsbereich 415 "Signal transduction."

Disclosures

None.

References

1. Carmeliet P. Mechanisms of angiogenesis and arteriogenesis. *Nat Med.* 2000;6:389–395.
2. Sato TN. Vascular development: molecular logic for defining arteries and veins. *Curr Opin Hematol.* 2003;10:131–135.
3. Wang HU, Chen ZF, Anderson DJ. Molecular distinction and angiogenic interaction between embryonic arteries and veins revealed by ephrin-B2 and its receptor Eph-B4. *Cell.* 1998;93:741–753.
4. Adams RH, Wilkinson GA, Weiss C, Diella F, Gale NW, Deutsch U, Risau W, Klein R. Roles of ephrinB ligands and EphB receptors in cardiovascular development: demarcation of arterial/venous domains, vascular morphogenesis, and sprouting angiogenesis. *Genes Dev.* 1999; 13:295–306.
5. Lawson ND, Weinstein BM. Arteries and veins: making a difference with zebrafish. *Nat Rev Genet.* 2002;3:674–682.
6. Yamashita JK. Differentiation and diversification of vascular cells from embryonic stem cells. *Int J Hematol.* 2004;80:1–6.
7. Rossant J, Hirashima M. Vascular development and patterning: making the right choices. *Curr Opin Genet Dev.* 2003;13:408–412.
8. Shawber CJ, Kitajewski J. Notch function in the vasculature: insights from zebrafish, mouse and man. *Bioessays.* 2004;26:225–234.

9. Zhong TP, Rosenberg M, Mohideen MA, Weinstein B, Fishman MC. gridlock, an HLH gene required for assembly of the aorta in zebrafish. *Science*. 2000;287:1820–1824.
10. Fischer A, Schumacher N, Maier M, Sendtner M, Gessler M. The Notch target genes Hey1 and Hey2 are required for embryonic vascular development. *Genes Dev*. 2004;18:901–911.
11. Daniel PB, Walker WH, Habener JF. Cyclic AMP signaling and gene regulation. *Annu Rev Nutr*. 1998;18:353–383.
12. Kitamura K, Kangawa K, Kawamoto M, Ichiki Y, Nakamura S, Matsuo H, Eto T. Adrenomedullin: a novel hypotensive peptide isolated from human pheochromocytoma. *Biochem Biophys Res Commun*. 1993;192: 553–560.
13. McLatchie LM, Fraser NJ, Main MJ, Wise A, Brown J, Thompson N, Solari R, Lee MG, Foord SM. RAMPs regulate the transport and ligand specificity of the calcitonin-receptor-like receptor. *Nature*. 1998;393: 333–339.
14. Shimosawa T, Ogihara T, Matsui H, Asano T, Ando K, Fujita T. Deficiency of adrenomedullin induces insulin resistance by increasing oxidative stress. *Hypertension*. 2003;41:1080–1085.
15. Shindo T, Kurihara Y, Nishimatsu H, Moriyama N, Kakoki M, Wang Y, Imai Y, Ebihara A, Kuwaki T, Ju KH, Minamino N, Kangawa K, Ishikawa T, Fukuda M, Akimoto Y, Kawakami H, Imai T, Morita H, Yazaki Y, Nagai R, Hirata Y, Kurihara H. Vascular abnormalities and elevated blood pressure in mice lacking adrenomedullin gene. *Circulation*. 2001;104:1964–1971.
16. Caron KM, Smithies O. Extreme hydrops fetalis and cardiovascular abnormalities in mice lacking a functional adrenomedullin gene. *Proc Natl Acad Sci U S A*. 2001;98:615–619.
17. Nishikawa SI, Nishikawa S, Hirashima M, Matsuyoshi N, Kodama H. Progressive lineage analysis by cell sorting and culture identifies FLK1+VE-cadherin+ cells at a diverging point of endothelial and hemopoietic lineages. *Development*. 1998;125:1747–1757.
18. Yamashita J, Itoh H, Hirashima M, Ogawa M, Nishikawa S, Yurugi T, Naito M, Nakao K, Nishikawa SI. Flk1-positive cells derived from embryonic stem cells serve as vascular progenitors. *Nature*. 2000;408: 92–96.
19. Yurugi-Kobayashi T, Itoh H, Yamashita J, Yamahara K, Hirai H, Kobayashi T, Ogawa M, Nishikawa S, Nishikawa SI, Nakao K. Effective contribution of transplanted vascular progenitor cells derived from embryonic stem cells to adult neovascularization in proper differentiation stage. *Blood*. 2003;101:2675–2678.
20. Schroeder T, Fraser M, Ogawa M, Nishikawa S, Oka C, Bornkamm GW, Nishikawa SI, Honjo T, Just U. Recombination signal sequence-binding protein Jkappa alters mesodermal cell fate decisions by suppressing cardiomyogenesis. *Proc Natl Acad Sci U S A*. 2003;100:4018–4023.
21. Schroeder T, Meier-Stiegen F, Schwanbeck R, Eilken H, Nishikawa S, Haler R, Schreiber S, Bornkamm GW, Nishikawa SI, Just U. Activated Notch1 alters differentiation of embryonic stem cells into mesodermal cell lineages at multiple stages of development. *Mech Dev*. In press.
22. Schroeder T, Just U. Notch signalling via RBP-J promotes myeloid differentiation. *EMBO J*. 2000;19:2558–2268.
23. Ohtsuka T, Imayoshi I, Shimojo H, Nishi E, Kageyama R, McConnell SK. Visualization of embryonic neural stem cells using Hes promoters in transgenic mice. *Mol Cell Neurosci*. doi 10.1016/j.mcn. 2005.09.006.
24. Yamashita JK, Takano M, Hiraoka-Kanie M, Shimazu C, Peishi Y, Yanagi K, Nakano A, Inoue E, Kita F, Nishikawa SI Prospective identification of cardiac progenitors by a novel single cell-based cardiomyocyte induction. *FASEB J*. 2005;19:1534–1536.
25. Ara T, Tokoyoda K, Okamoto R, Pandelakis AK, Nagasawa T. The role of CXCL12 in the organ-specific process of artery formation. *Blood*. 2005;105:3155–3161.
26. Hippenstiel S, Witzenrath M, Schmeck B, Hocke A, Krisp M, Krüll M, Seybold J, Seeger W, Rascher W, Schütte H, Suttorp N. Adrenomedullin reduces endothelial hyperpermeability. *Circ Res*. 2002;91:618–625.
27. Fuller T, Korff T, Kilian A, Dandekar G, Augustin HG. Forward EphB4 signaling in endothelial cells controls cellular repulsion and segregation from ephrinB2 positive cells. *J Cell Sci*. 2003;116:2461–2470.
28. You LR, Lin FJ, Lee CT, DeMayo FJ, Tsai MJ, Tsai SY. Suppression of Notch signaling by the COUP-TFII transcription factor regulates vein identity. *Nature*. 2005;435:98–104.
29. Herzog Y, Guttmann-Raviv N, Neufeld G. Segregation of arterial and venous markers in subpopulations of blood islands before vessel formation. *Dev Dyn*. 2005;232:1047–1055.
30. Tachibana K, Hirota S, Iizasa H, Yoshida H, Kawbata K, Kataoka Y, Kitamura Y, Matsushima K, Yoshida N, Nishikawa SI, Kishimoto T, Nagasawa T. The chemokine receptor CXCR4 is essential for vascularization of the gastrointestinal tract. *Nature*. 1998;393:591–594.
31. Mumm JS, Kopan R. Notch signaling: from the outside in. *Dev Biol*. 2000;228:151–165.
32. Zhong TP, S. Childs, J.P. Leu, Fishman. MC. Gridlock signalling pathway fashions the first embryonic artery. *Nature*. 2001;414: 216–220.
33. Lawson ND, Scheer N, Pham VN, Kim CH, Chitnis AB, Campos-Ortega JA, Weinstein BM. Notch signaling is required for arterial-venous differentiation during embryonic vascular development. *Development*. 2001; 128:3675–3683.
34. Duarte A, Hirashima M, Benedito R, Trindade A, Diniz P, Bekman E, Costa L, Henrique D, Rossant J. Dosage-sensitive requirement for mouse Dll4 in artery development. *Genes Dev*. 2004;18:2474–2478.
35. Krebs LT, Shutter JR, Tanigaki K, Honjo T, Stark KL, Gridley T. Haploinsufficient lethality and formation of arteriovenous malformations in Notch pathway mutants. *Genes Dev*. 2004;18:2469–2473.
36. Uyttendaele H, Ho J, Rossant J, Kitajewski J. Vascular patterning defects associated with expression of activated Notch4 in embryonic endothelium. *Proc Natl Acad Sci U S A*. 2001;98:5643–5648.
37. Miyashita K, Itoh H, Sawada N, Fukunaga Y, Sone M, Yamahara K, Yurugi-Kobayashi T, Park K, Nakao K. Adrenomedullin provokes endothelial Akt activation and promotes vascular regeneration both in vitro and in vivo. *FEBS Lett*. 2003;544:86–92.
38. Iwase T, Nagaya N, Fujii T, Itoh T, Ishibashi-Ueda H, Yamagishi M, Miyatake K, Matsumoto T, Kitamura S, Kangawa K. Adrenomedullin enhances angiogenic potency of bone marrow transplantation in a rat model of hindlimb ischemia. *Circulation*. 2005;111:356–362.
39. Mitsuda N, Ohkubo N, Tamatani M, Lee YD, Taniguchi M, Namikawa K, Kiyama H, Yamaguchi A, Sato N, Sakata K, Ogihara T, Vitek MP, Tohyama M. Activated cAMP-response element-binding protein regulates neuronal expression of presenilin-1. *J Biol Chem*. 2001;276: 9688–9698.
40. Williams CK, Li JL, Murga M, Harris AL, Tosato G. Up-regulation of the Notch ligand Delta-like 4 inhibits VEGF-induced endothelial cell function. *Blood*. 2006;107:931–939.
41. Darland DC, Massingham LJ, Smith SR, Piek E, Saint-Geniez M, D'Amore PA. Pericyte production of cell-associated VEGF is differentiation-dependent and is associated with endothelial survival. *Dev Biol*. 2003;264:275–288.
42. Montuenga LM, Mariano K, Prentice MA, Cuttitta F, Jakowlew SB. Coordinate expression of transforming growth factor-beta1 and adrenomedullin in rodent embryogenesis. *Endocrinology*. 1998;139: 3946–3957.
43. Mukouyama YS, Shin D, Britsch S, Taniguchi M, Anderson DJ. Sensory nerves determine the pattern of arterial differentiation and blood vessel branching in the skin. *Cell*. 2002;109:693–705.
44. Hobara N, Nakamura A, Ohtsuka A, Narasaki M, Shibata K, Gomoita Y, Kawasaki H. Distribution of adrenomedullin-containing perivascular nerves in the rat mesenteric artery. *Peptides*. 2004;25:589–599.

Am J Physiol Endocrinol Metab 290: E583–E590, 2006.
First published October 25, 2005; doi:10.1152/ajpendo.00395.2005.

Low-intensity contraction activates the α1-isoform of 5′-AMP-activated protein kinase in rat skeletal muscle

Taro Toyoda,[1] Satsuki Tanaka,[2] Ken Ebihara,[2] Hiroaki Masuzaki,[2] Kiminori Hosoda,[2] Kenji Sato,[3] Tohru Fushiki,[1] Kazuwa Nakao,[2] and Tatsuya Hayashi[4]

[1]*Laboratory of Nutrition Chemistry, Division of Food Science and Biotechnology, Graduate School of Agriculture, Kyoto University;* [2]*Department of Medicine and Clinical Science, Graduate School of Medicine, Kyoto University;* [3]*Laboratory of Food Science, Department of Food Sciences and Nutritional Health, Kyoto Prefectural University; and* [4]*Laboratory of Sports and Exercise Medicine, Graduate School of Human and Environmental Studies, Kyoto University, Kyoto, Japan*

Submitted 23 August 2005; accepted in final form 20 October 2005

Toyoda, Taro, Satsuki Tanaka, Ken Ebihara, Hiroaki Masuzaki, Kiminori Hosoda, Kenji Sato, Tohru Fushiki, Kazuwa Nakao, and Tatsuya Hayashi. Low-intensity contraction activates the α1-isoform of 5′-AMP-activated protein kinase in rat skeletal muscle. *Am J Physiol Endocrinol Metab* 290: E583–E590, 2006. First published October 25, 2005; doi:10.1152/ajpendo.00395.2005.—Skeletal muscle expresses two catalytic subunits, α1 and α2, of the 5′-AMP-activated protein kinase (AMPK), which has been implicated in contraction-stimulated glucose transport and fatty acid oxidation. Muscle contraction activates the α2-containing AMPK complex (AMPKα2), but this activation may occur with or without activation of the α1-containing AMPK complex (AMPKα1), suggesting that AMPKα2 is the major isoform responsible for contraction-induced metabolic events in skeletal muscle. We report for the first time that AMPKα1, but not AMPKα2, can be activated in contracting skeletal muscle. Rat epitrochlearis muscles were isolated and incubated in Krebs-Ringer bicarbonate buffer containing pyruvate. In muscles stimulated to contract at a frequency of 1 and 2 Hz during the last 2 min of incubation, AMPKα1 activity increased twofold and AMPKα2 activity remained unchanged. Muscle stimulation did not change the muscle AMP concentration or the AMP-to-ATP ratio. AMPK activation was associated with increased phosphorylation of Thr^{172} of the α-subunit, the primary activation site. Muscle stimulation increased the phosphorylation of acetyl-CoA carboxylase (ACC), a downstream target of AMPK, and the rate of 3-*O*-methyl-D-glucose transport. In contrast, increasing the frequency (≥5 Hz) or duration (≥5 min) of contraction activated AMPKα1 and AMPKα2 and increased AMP concentration and the AMP/ATP ratio. These results suggest that *1*) AMPKα1 is the predominant isoform activated by AMP-independent phosphorylation in low-intensity contracting muscle, *2*) AMPKα2 is activated by an AMP-dependent mechanism in high-intensity contracting muscle, and *3*) activation of each isoform enhances glucose transport and ACC phosphorylation in skeletal muscle.

exercise; twitch; glucose transport; acetyl-coenzyme A carboxylase; β-oxidation

EXERCISE TRIGGERS AN INCREASE in glucose and fatty acid utilization in contracting muscle. 5′-AMP-activated protein kinase (AMPK) is an important signaling intermediary in this increased use of substrates. AMPK activation leads to contraction-stimulated glucose transport in skeletal muscle (21, 34) and is thought to be involved in the regulation of fatty acid oxidation by phosphorylation of acetyl-CoA carboxylase (ACC) (49). Phosphorylation of AMPK by its upstream kinase AMPK kinase (AMPKK) increases the activity of AMPK (26, 47). AMPK activity also increases in response to an increase in AMP concentration or in the AMP-to-ATP ratio (1, 2, 9, 33). Binding of AMP directly activates AMPK through allosteric modification and makes AMPK a better substrate for AMPKK (33). AMPK is a heterotrimeric kinase, consisting of a catalytic α-subunit (1) and two regulatory subunits, β and γ (6). Two distinct α-isoforms (α1, α2) exist in mammals (42), and the α-isoform determines the enzyme characteristics, such as different conditions of activation in contracting muscle.

The α2-containing AMPK complex (AMPKα2) is considered the major AMPK isoform responsible for the metabolic changes in contracting skeletal muscle. A single bout of moderate-intensity exercise at ~70% of maximal O_2 uptake ($\dot{V}O_{2max}$), which increases glucose transport and ACC phosphorylation, significantly activates AMPKα2, but not the α1-containing AMPK complex (AMPKα1), in human vastus lateralis muscle (12, 44, 50). In rat skeletal muscle, electrical stimulation (ES) of the sciatic nerve to produce periodic muscle contractions (46) and voluntary treadmill running exercise (35) increase only AMPKα2 activity, which is accompanied by increased glucose transport and ACC phosphorylation. Whole body AMPKα2 knockout mice exhibit impaired whole body insulin sensitivity and abolished stimulation of glucose transport into skeletal muscle induced by 5-aminoimidazole-4-carboxamide-1-β-D-ribofuranoside (AICAR), an AMPK activator (27). These results suggest that lower-intensity exercise or muscle contraction activates AMPKα2 more than AMPKα1 and that activation of AMPKα2 alone is sufficient to increase glucose transport and ACC phosphorylation. An acute bout of exercise increases the nuclear content of AMPKα2 but not of AMPKα1 (31). These findings indicate the importance of AMPKα2 in contraction-induced metabolic changes in skeletal muscle.

AMPKα1 has also been implicated in skeletal muscle metabolism. Earlier studies suggested that AMPKα1 activity increases only in response to high-intensity exercise, such as a 30-s all-out sprint exercise in humans (3). High-intensity contractions, such as electrically induced tetanic contractions, increase AMPKα1 activity in isolated rat skeletal muscle (35). In contrast, recent reports indicate that AMPKα1 activity also increases in response to moderate-intensity exercise (4, 5). One study reported a small but significant increase in AMPKα1

Address for reprint requests and other correspondence: T. Hayashi, Laboratory of Sports and Exercise Medicine, Graduate School of Human and Environmental Studies, Kyoto University, Yoshida-nihonmatsu-cho, Sakyo-ku, Kyoto, 606-8501, Japan (e-mail: tatsuya@kuhp.kyoto-u.ac.jp).

The costs of publication of this article were defrayed in part by the payment of page charges. The article must therefore be hereby marked "*advertisement*" in accordance with 18 U.S.C. Section 1734 solely to indicate this fact.

when exercise intensity increased from 40 to 60% of $\dot{V}O_{2max}$ in a progressive incremental exercise protocol (4). Repeated higher-intensity exercise at 85% of $\dot{V}O_{2max}$ also increases AMPKα1 activity in humans (5). These reports suggest that AMPKα1 can be activated by exercise at a lower intensity than previously thought necessary.

The pharmacological activation of AMPKα1 increases glucose transport and ACC phosphorylation, suggesting that AMPKα1 is also involved in glucose and fatty acid metabolism (22, 45). We (45) have previously shown that AMPKα1 is activated by hydrogen peroxide (H_2O_2) in isolated rat epitrochlearis muscle and that this is accompanied by increased glucose transport and ACC phosphorylation. Sodium nitroprusside (SNP) stimulates predominantly AMPKα1 activity and enhances glucose transport in isolated rat skeletal muscle (22). In whole body AMPKα1 knockout mice, contraction-induced glucose transport decreases slightly but significantly in the soleus muscle (27), a muscle that normally has an abundance of α1-subunit in wild-type animals (48). Moreover, the protein content of α1-subunit, but not α2-subunit, increases after 3–8 wk of endurance training in human (10, 29) and rat (38) skeletal muscle, and the protein content of α1-subunit is markedly higher in well-trained than in untrained individuals (36). These findings raise the possibility that AMPKα1 may play an important role in exercise-induced metabolic changes in skeletal muscle.

To our knowledge, no one has studied whether increased AMPKα1 activation increases glucose transport and ACC phosphorylation in wild-type skeletal muscle during contraction. In most previous studies, coactivation of AMPKα2 might have obscured the role of AMPKα1 in contracting skeletal muscle. The purpose of this study was to clarify the metabolic role of AMPKα1 in contracting skeletal muscle. We first determined the stimulation parameters that selectively increase the kinase activity of AMPKα1 but not AMPKα2. Because tetanic contractions stimulate both AMPKα1 and AMPKα2, even when the stimulation duration is for 10 s (35), we used "twitch" contractions to precisely manipulate the contraction intensity.

MATERIALS AND METHODS

Experimental animals. Male Sprague-Dawley rats weighing 100 g were purchased from Clea Japan (Tokyo, Japan). Animals were housed in an animal room maintained at 23°C with a 12:12-h light-dark cycle and fed a standard laboratory diet (Certified Diet MF; Oriental Koubo, Tokyo, Japan) and water ad libitum. Rats were fasted overnight before the experiments and were randomly assigned to the experimental groups. All protocols for animal use and euthanasia were reviewed and approved by the Institute of Laboratory Animals, Graduate School of Medicine, Kyoto University, Japan.

Materials. Pyruvate was purchased from Nacalai Tesque (Kyoto, Japan). The SAMS peptide (HMRSAMSGLHLVKRR) was provided by A. Otaka (Graduate School of Pharmaceutical Sciences, Kyoto University) (45). 3-*O*-[methyl-^{3}H]-D-glucose (3-MG) was purchased from American Radiolabeled Chemicals (St. Louis, MO). [γ-^{32}P]ATP and D-[1-^{14}C]mannitol were obtained from NEN Life Science Products (Boston, MA). P81 filter paper was obtained from Whatman International (Maidstone, UK). Protein A-Sepharose CL-4B was from Amersham Biosciences (Uppsala, Sweden). All other reagents were of analytical grade and obtained from Sigma (St. Louis, MO), unless otherwise stated.

Antibodies. AMPK antibodies were raised in rabbit against isoform-specific peptides derived from the amino acid sequences of rat α1 (residues 339–358) or α2 (residues 490–514) (45). Peptides used for immunization were provided by A. Otaka. Immunized sera were used as antibodies.

Muscle treatment. Rat epitrochlearis muscles were treated as described previously, with modifications (21, 45). Rats were killed by cervical dislocation, and the muscles were rapidly removed. When anesthetized, rats were treated with pentobarbital sodium (50 mg/kg body wt ip), and the muscles were isolated either with or without cervical dislocation. Isolated muscles were frozen immediately after isolation or incubated as follows. Both ends of each muscle were tied with sutures (silk 3-0; Natsume Seisakusho, Tokyo, Japan) and the muscles were mounted on an incubation apparatus with the resting tension set to 0.5 g. The buffers were continuously gassed with 95% O_2-5% CO_2 and maintained at 37°C. Muscles were preincubated in 7 ml of Krebs-Ringer bicarbonate buffer (KRB) (in mM: 117 NaCl, 4.7 KCl, 2.5 $CaCl_2$, 1.2 KH_2PO_4, 1.2 $MgSO_4$, 24.6 $NaHCO_3$) containing 2 mM pyruvate (KRBP) for 40 min. The muscles were then incubated for 60 min in KRBP. For the twitch contraction treatments, muscles were stimulated during the last 0.5, 1, 2, 5, and 8 min of the incubation period at various frequencies (0.5–8 Hz) with 0.1-ms square-wave 50-V pulses. For the tetanic contraction treatments, muscles were stimulated during the last 10 min of the incubation period (train rate = 1/min, train duration = 10 s, pulse rate = 100 pulses/s, duration = 0.1 ms, volts = 50 V). The muscles were then used for the measurement of glucose uptake (see *3-MG transport*), or immediately frozen in liquid nitrogen and subsequently analyzed for AMP, ATP (see *Assays for metabolites*), and isoform-specific AMPK activity, or used for Western blot analysis.

Western blotting and isoform-specific AMPK activity assay. Muscles were homogenized in ice-cold lysis buffer (1:40 wt/vol) containing 20 mM Tris·HCl (pH 7.4), 1% Triton X, 50 mM NaCl, 250 mM sucrose, 50 mM NaF, 5 mM sodium pyrophosphate, 2 mM dithiothreitol, 4 mg/l leupeptin, 50 mg/l trypsin inhibitor, 0.1 mM benzamidine, and 0.5 mM phenylmethylsulfonyl fluoride and centrifuged at 20,000 *g* for 40 min at 4°C. For Western blot analysis, denatured lysates (10 μg of protein) were separated on either 7% polyacrylamide gel for phosphorylated AMPK or 5% gel for phosphorylated ACC. Proteins were then transferred to polyvinylidene difluoride membranes (PolyScreen; NEN Life Science Products) at 100 V for 1 h. Membranes were blocked with Block Ace (Yukijirushi Nyugyo, Sapporo, Japan) overnight at 4°C and were then incubated with phosphospecific antibodies directed against AMPKα Thr^{172} (Cell Signaling Technology, Beverly, MA) or against ACC Ser^{79} (Upstate Biotechnology, Lake Placid, NY). The membranes were then washed, reacted with anti-rabbit IgG coupled to peroxidase, and developed with enhanced chemiluminescence reagents according to the manufacturer's instructions (Amersham, Buckinghamshire, UK). The signal on the blot was detected and quantified with a Lumino-Image Analyzer LAS-1000 System (Fuji Photo Film, Tokyo, Japan). For the AMPK activity assay, the supernatants (100 μg of protein) were immunoprecipitated with isoform-specific antibodies directed against the α1 or α2 catalytic subunits of AMPK and protein A-Sepharose beads (21, 45). Immunoprecipitates were washed twice both in lysis buffer and in wash buffer (240 mM HEPES and 480 mM NaCl). Kinase reactions were performed in (in mM) 40 HEPES (pH 7.0), 0.1 SAMS peptide, 0.2 AMP, 80 NaCl, 0.8 dithiothreitol, 5 $MgCl_2$, 0.2 ATP (2 μCi of [γ-^{32}P]ATP), in a final volume of 40 μl for 20 min at 30°C. At the end of the reaction, a 15-μl aliquot was removed and spotted onto Whatman P81 paper. The papers were washed six times in 1% phosphoric acid and once in acetone. ^{32}P incorporation was quantitated with a scintillation counter, and kinase activity was expressed as fold increases relative to the basal samples.

Assays for metabolites. Frozen muscles were homogenized in 0.2 M $HClO_4$ (3:25 wt/vol) in an ethanol-dry ice bath and centrifuged at